Reactions of ^{t}BuC≡P with Cyclooctatetraene-Supported Titanium Imido Complexes

F. Geoffrey N. Cloke,*,† Jennifer C. Green,*,‡ Nilay Hazari,‡ Peter B. Hitchcock,† Philip Mountford,*,‡ John F. Nixon,*,† and D. James Wilson†

The Department of Chemistry, School of Life Sciences, University of Sussex, Brighton BN1 9QJ, U.K., and Inorganic Chemistry Laboratory, University of Oxford, South Parks Road, Oxford OX1 3QR, U.K.

Received March 29, 2006

Reaction of the pseudo two-coordinate titanium imido complexes [Ti(N^{t}Bu)(COT)] (**1**; COT = η^8-C_8H_8) and [Ti(N^{t}Bu)(COT″)] (**2**; COT″ = η^8-1,4-$C_8H_6(SiMe_3)_2$) with 2 equiv of ^{t}BuC≡P generated the new complexes [Ti{N(^{t}Bu)PC(^{t}Bu)PC(^{t}Bu)}(COT)] (**4**) and [Ti{N(^{t}Bu)PC(^{t}Bu)PC(^{t}Bu)}(COT″)] (**5**), respectively. Complex **4** was crystallographically characterized, and a density functional theory (DFT) study combined with photoelectron (PE) spectroscopy revealed this apparently 20-valence-electron species to contain a HOMO which is almost entirely ligand-based. In contrast, the organic compound N(Ar)-$P_2C_2{}^{t}Bu_2$ (**6**), which incorporates a 1,2,4-azadiphosphole ring, was the only isolated product from the reaction of the arylimido species [Ti(NAr)(COT)] (**3**; Ar = 2,6-$^{i}Pr_2C_6H_3$) with an excess of ^{t}BuC≡P. DFT studies indicated that the mechanisms for the formation of compounds **4**−**6** are similar. Initially, one molecule of ^{t}BuC≡P undergoes a [2 + 2] cycloaddition with [Ti(NR)(COT)] to form [Ti{N(R)PC(^{t}Bu)}(COT)], which contains a Ti−C bond. Subsequently, a second molecule of ^{t}BuC≡P reacts with [Ti{N(R)PC(^{t}Bu)}(COT)] to form [Ti{N(R)PC(^{t}Bu)PC(^{t}Bu)}(COT)]. When R = 2,6-$^{i}Pr_2C_6H_3$ or a substituent which is less sterically bulky, the formation of a heterocyclic ring such as N(Ar)$P_2C_2{}^{t}Bu_2$ (**6**) is favored. However, when R = ^{t}Bu, it is sterically unfavorable to form such a ring and thus compound **4** is stable.

Introduction

Over the last 15 years there has been significant interest in the chemistry of terminal titanium imido complexes of the type $(L)_nTi{=}NR$ (where $(L)_n$ represents a supporting ligand set and R is generally an alkyl or aryl group).[1−6] Complexes of this type were first structurally characterized in 1990,[7,8] and it has subsequently been shown that they have proven potential in materials chemistry (as a source of TiN),[9−12] as intermediates in hydroamination,[13−20] and as catalysts for olefin polymerization (Ti=NR acting as a "spectator ligand").[21,22] However, it is the ability of the Ti=NR bond to act as a reactive site toward unsaturated substrates that is particularly attractive. It has been established that titanium imides react with many organic substrates, including alkenes, allenes, alkynes, heterocumulenes, nitriles, isonitriles, and isocyanates, and in many cases these reactions result in the formation of both novel organic products and metal-containing species.[6]

Since the report by Regitz and co-workers describing the synthesis of 1,3,5-triphosphabenzenes through the reaction of ^{t}BuC≡P with vanadium imido species, there has been interest in the reactions of imides with phosphaalkynes.[23] Previously, we have shown that the sterically hindered titanium imide [Ti(N^{t}Bu){MeC(C_5H_4N-2)(CH_2NSiMe_3)$_2$}(py)] reacts with 1 equiv of ^{t}BuC≡P to generate the [2 + 2] cycloaddition product [Ti{N(^{t}Bu)PC(^{t}Bu)}{MeC(C_5H_4N-2)(CH_2NSiMe_3)$_2$}] (**A**)[24] and that the zirconium chalcogenide complexes [(η^5-$(C_5Me_5)_2$)Zr(=E)] (E = S, Se) (the Zr=S or Zr=Se bond is isoelectronic

* To whom correspondence should be addressed. E-mail: jennifer.green@chem.ox.ac.uk (J.C.G.).
† University of Sussex.
‡ University of Oxford.

(1) Wigley, D. E. *Prog. Inorg. Chem.* **1994**, *42*, 239.
(2) Mountford, P. *Chem. Commun.* **1997**, 2127.
(3) Gade, L. H.; Mountford, P. *Coord. Chem. Rev.* **2001**, *216−217*, 65.
(4) Radius, U. *Z. Anorg. Allg. Chem.* **2004**, *630*, 957.
(5) Bolton, P. D.; Mountford, P. *Adv. Synth. Catal.* **2005**, *347*, 355.
(6) Hazari, N.; Mountford, P. *Acc. Chem. Res.* **2005**, *38*, 839.
(7) Roesky, H. W.; Voelker, H.; Witt, M.; Noltemeyer, M. *Angew. Chem., Int. Ed. Engl.* **1990**, *29*, 669.
(8) Hill, J. E.; Profilet, R. D.; Fanwick, P. E.; Rothwell, I. P. *Angew. Chem., Int. Ed. Engl.* **1990**, *29*, 664.
(9) Winter, C. H.; Sheridan, P. H.; Lewkebandara, T. S.; Heeg, M. J.; Proscia, J. W. *J. Am. Chem. Soc.* **1992**, *114*, 1095.
(10) Lewkebandara, T. S.; Sheridan, P. H.; Heeg, M. J.; Rheingold, A. L.; Winter, C. H. *Inorg. Chem.* **1994**, *33*, 5879.
(11) McKarns, P. J.; Yap, G. P. A.; Rheingold, A. L.; Winter, C. H. *Inorg. Chem.* **1996**, *35*, 5968.
(12) Carmalt, C. J.; Newport, A. C.; Parkin, I. P.; Mountford, P.; Sealey, A. J.; Dubberley, S. R. *J. Mater. Chem.* **2003**, *13*, 84.
(13) Pohlki, F.; Doye, S. *Chem. Soc. Rev.* **2003**, *32*, 104.
(14) Li, Y.; Shi, Y.; Odom, A. L. *J. Am. Chem. Soc.* **2004**, *126*, 1794.
(15) Nobis, M.; Driessen-Hölscher, B. *Angew. Chem., Int. Ed.* **2001**, *40*, 3983.
(16) Tillack, A.; Jiao, H.; Garcio-Castro, I.; Hartung, C. G.; Beller, M. *Chem. Eur. J.* **2004**, *10*, 2409.
(17) Ackermann, L.; Bergman, R. G.; Loy, R. N. *J. Am. Chem. Soc.* **2003**, *125*, 11956.
(18) Bytschkov, I.; Doye, S. *Eur. J. Inorg. Chem.* **2003**, *6*, 935.
(19) McGrane, P. L.; Jensen, M.; Livinghouse, T. *J. Am. Chem. Soc.* **1992**, *114*, 5459.
(20) McGrane, P. L.; Livinghouse, T. *J. Am. Chem. Soc.* **1993**, *115*, 11485.
(21) Adams, N.; Arts, H. J.; Bolton, P. D.; Cowell, D.; Dubberley, S. R.; Friederichs, N.; Grant, C.; Kranenbrug, M.; Sealey, A. J.; Wang, B.; Wilson, P. J.; Cowley, A. R.; Mountford, P.; Schröder, M. *Chem. Commun.* **2004**, 434.
(22) Bigmore, H. R.; Dubberley, S. R.; Kranenburg, M.; Lawrence, S. C.; Sealey, A. J.; Selby, J. D.; Zuideveld, M.; Cowley, A. R.; Mountford, P. *Chem. Commun.* **2006**, 436.
(23) Tabellion, F.; Nachbauer, A.; Leininger, S.; Peters, C.; Preuss, F.; Regitz, M. *Angew. Chem., Int. Ed.* **1998**, *37*, 1233.
(24) Pugh, S. M.; Trösch, D. J. M.; Wilson, D. J.; Bashall, A.; Cloke, F. G. N.; Gade, L. H.; Hitchcock, P. B.; McPartlin, M.; Nixon, J. F.; Mountford, P. *Organometallics* **2000**, *19*, 3205.

10.1021/om060273o CCC: $33.50
Publication on Web 06/15/2006

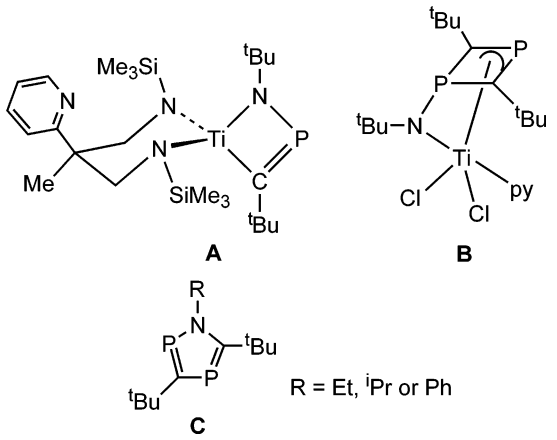

with Ti═NR) also undergo [2 + 2] cycloaddition reactions with ^{t}BuC≡P.[25] In contrast, reaction of 2 equiv of ^{t}BuC≡P with the less sterically demanding imido complex [Ti(N^{t}Bu)Cl$_2$(py)$_3$] results in the formation of the two-step [2 + 2] cycloaddition product [TiCl$_2${N(^{t}Bu)PC(^{t}Bu)PC(^{t}Bu)}(py)] (**B**).[26] Interestingly, the products of the reactions between complexes of the type [Ti(NR)Cl$_2$(py)$_3$] and ^{t}BuC≡P are dependent on the identity of the substituent on the imido ligand, and when R = Ph, Et, ^{i}Pr, the compounds N(R)P$_2$C$_2$^{t}Bu$_2$ (**C**), which contain an aromatic 1,2,4-azadiphosphole ring, are the only isolated products.[27]

Recently, we reported the syntheses and reactivity of a series of highly unusual pseudo two-coordinate titanium imido cyclooctatetraenyl complexes of the types [Ti(NR)(COT)] and [Ti(NR)(COT″)] (R = alkyl, aryl, COT = η^8-C$_8$H$_8$, COT″ = η^8-1,4-C$_8$H$_6$(SiMe$_3$)$_2$).[28,29] Both the geometry and the electronic structure of these complexes are unique in early-transition-metal chemistry, and in some cases they displayed unusual reactivity. In this contribution we report the reactions of the pseudo two-coordinate species [Ti(N^{t}Bu)(COT)] (**1**), [Ti(N^{t}Bu)(COT″)] (**2**), and [Ti(NAr)(COT)] (**3**; Ar = 2,6-^{i}Pr$_2$C$_6$H$_3$) with the phosphaalkyne ^{t}BuC≡P and a computational investigation of the mechanism of these reactions. In addition, the electronic structures of the products of these reactions have been studied using both DFT calculations and gas-phase photoelectron spectroscopy.

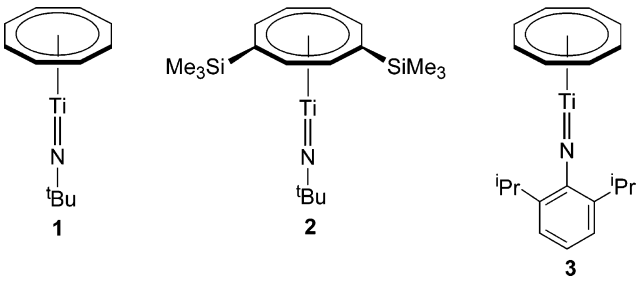

Results and Discussion

Reactions of [Ti(N^{t}Bu)(COT)] (1) and [Ti(N^{t}Bu)(COT″)] (2) with ^{t}BuC≡P. The titanium imido COT starting materials

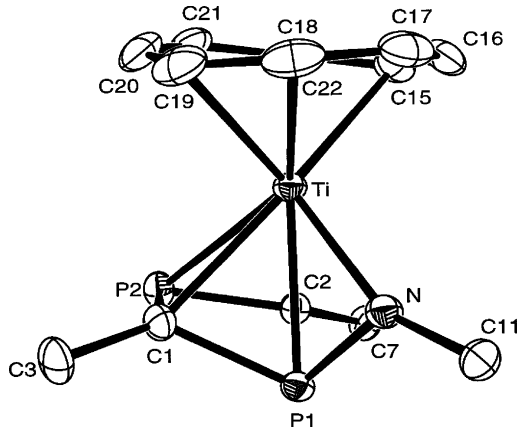

Figure 1. Displacement ellipsoid plot of [Ti{N(^{t}Bu)PC(^{t}Bu)PC(^{t}Bu)}(COT)] (**4**) (30% probability). H atoms and selected C atoms are omitted for clarity.

Table 1. Comparison between Selected Experimental and Calculated Bond Lengths (Å) and Angles (deg) for [Ti{N(^{t}Bu)PC(^{t}Bu)PC(^{t}Bu)}(COT)] (4)

bond length or angle	exptl	calcd
Ti−P(1)	2.437(10)	2.43
Ti−N	2.041(2)	2.01
Ti−P(2)	2.6964(7)	2.66
Ti−C(1)	2.272(2)	2.24
N−P(1)	1.659(2)	1.67
C(1)−P(1)	1.837(2)	1.83
C(1)−C(2)	1.763(2)	1.78
C(2)−P(1)	1.825(2)	1.82
C(2)−P(2)	1.763(2)	1.77
N−P(1)−C(1)	104.33(10)	104
C(1)−P(2)−C(2)	84.97(10)	84
Ti−N−C(11)	152.49(14)	152
P(1)−C(1)−C(3)	126.6(2)	127
P(2)−C(2)−C(7)	129.8(2)	130

[Ti(N^{t}Bu)(COT)] (**1**) and [Ti(N^{t}Bu)(COT″)] (**2**) were prepared according to previously described routes.[28] Addition of 2 equiv of ^{t}BuC≡P to either **1** or **2** in toluene gave a dark brown solution. After standard workup and recrystallization from pentane, clean samples of [Ti{N(^{t}Bu)PC(^{t}Bu)PC(^{t}Bu)}(COT)] (**4**) and [Ti{N(^{t}Bu)PC(^{t}Bu)PC(^{t}Bu)}(COT″)] (**5**) were isolated as black solids in yields of 71 and 75%, respectively (eq 1). Compounds **4** and **5** were fully characterized.

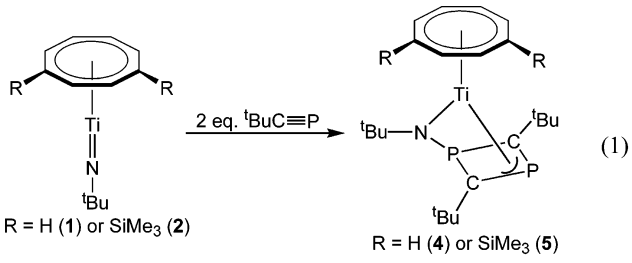

(1)

Crystals of [Ti{N(^{t}Bu)PC(^{t}Bu)PC(^{t}Bu)}(COT)] (**4**) suitable for X-ray diffraction analysis were obtained from a cooled (−18 °C) pentane solution of **4**. The molecular structure is shown in Figure 1, and selected bond distances and angles are presented in Table 1 together with those calculated by DFT analysis (vide infra). The most interesting feature of the structure of **4** is the TiC$_2$P$_2$N core, in which two molecules of ^{t}BuC≡P are bonded together to form a 1,3-diphosphacyclobutadiene unit, whose P(1) atom is σ-bonded to the nitrogen of the imide function. The C(1)−P(1) (1.837(2) Å) and C(2)−P(1) (1.825(2) Å) distances are similar and are longer than the C(1)−P(2) (1.763(2) Å) and

(25) d'Arbeloff-Wilson, S. E.; Hitchcock, P. B.; Nixon, J. F.; Kawaguchi, H.; Tatsumi, K. *J. Organomet. Chem.* **2003**, *672*, 1.
(26) Cloke, F. G. N.; Hitchcock, P. B.; Nixon, J. F.; Wilson, D. J.; Mountford, P. *Chem. Commun.* **1999**, 661.
(27) Cloke, F. G. N.; Hitchcock, P. B.; Nixon, J. F.; Wilson, D. J.; Tabellion, F.; Fischbeck, U.; Preuss, F.; Regitz, M.; Nyulaszi, L. *Chem. Commun.* **1999**, 2363.
(28) Dunn, S. C.; Hazari, N.; Jones, N. M.; Moody, A. G.; Blake, A. J.; Cowley, A. R.; Green, J. C.; Mountford, P. *Chem. Eur. J.* **2005**, *11*, 2111.
(29) Dunn, S. C.; Hazari, N.; Cowley, A. R.; Green, J. C.; Mountford, P. *Organometallics* **2006**, 1755.

C(2)−P(2) (1.763(2) Å) bond lengths, which are identical. The formal description of the coordination of the C_2P_2 core to the titanium center is unclear, although one possible representation may involve an η^3 interaction between the 2-phosphaallyl fragment of the C_2P_2 ring and Ti, along with donation from the lone pair on P(1) to the metal center. The Ti−N bond length in **4** (Ti−N = 2.041(2) Å) is considerably elongated when compared with that in the starting imido complex **1** (Ti−N in **1** = 1.699(6) Å),[28] which indicates that the Ti−N bond order has been reduced. The Ti−N−C(11) bond angle (152.49(14)°) is intermediate between values expected for sp and sp^2 hybridization of nitrogen.[30] Overall, the TiC_2P_2N core is extremely similar to that observed in [$TiCl_2${N(ᵗBu)PC(ᵗBu)-PC(ᵗBu)}(py)], which is the only other example of a complex of this type.[26]

Although all of the bond distances of the cyclooctatetraenyl ring are approximately equal (average 1.397 Å), the ring is not planar but is puckered, which gives rise to the observed variation in the Ti−C bond distances (Ti−C_8H_8 distances vary from 2.347(2) to 2.493(2) Å). Deviations from planarity in η^8-COT rings are unusual,[28] and in this case the puckering is probably due to the unsymmetrical core of the P_2C_2N ligand.

The ^{31}P NMR spectroscopic data for **4** are in agreement with the solid-state molecular structure. The $^{31}P\{^1H\}$ NMR spectrum displays two doublets (δ 215.4, −190.8 ppm), as expected for the two chemically nonequivalent P nuclei ($^2J_{P-P}$ = 38.7 Hz). The high-field resonance is readily assigned to the saturated phosphorus atom and is broadened due to coupling to quadrapolar ^{14}N. The quaternary ring carbons display a characteristic four-line second-order resonance (δ 185.3 ppm) in the $^{13}C\{^1H\}$ NMR spectrum, which is characteristic of the TiP_2C_2N core in **4** (vide supra). The NMR data for **5** are consistent with those of **4**, and thus, by analogy, **5** is proposed to have a similar structure. These reactions highlight the known similarities in the reactivities of complexes **1** and **2**, which are related to their almost identical electronic structures.[28]

Even though the TiP_2C_2N core in compound **4** (and by analogy **5**) is spatially open to attack, no further reaction was observed with an excess of ᵗBuC≡P in toluene at reflux for 24 h. Clearly, the reactions of **1** and **2** with ᵗBuC≡P are similar to the reaction between [Ti(NᵗBu)Cl_2(py)$_3$] and ᵗBuC≡P, which also results in the addition of two molecules of the phosphaalkyne to the imide and the formation of the complex [$TiCl_2${N(ᵗBu)PC(ᵗBu)PC(ᵗBu)}(py)].[26] The common TiC_2P_2N core presumably has some structural significance in this type of reaction.

Reactions between [Ti(N-2,6-^{i}Pr$_2$C$_6$H$_3$)(COT)] (3) and ᵗBuC≡P. In contrast to the reactions of **1** and **2** with ᵗBuC≡P, no metal-containing species were characterized or isolated from the reaction of [Ti(NAr)(COT)] (**3**; Ar = 2,6-^{i}Pr$_2$C$_6$H$_3$) and an excess (approximately 4 equiv) of ᵗBuC≡P. Instead, the organic compound N(Ar)P_2C_2ᵗBu$_2$ (**6**), which incorporates a 1,2,4-azadiphosphole ring, was isolated in 30% yield (eq 2). The reaction was extremely slow at room temperature, and an excess of ᵗBuC≡P was required to ensure all of starting complex **3** was consumed. A significant quantity of crude N(Ar)P_2C_2ᵗBu$_2$ (**6**) was lost during the purification process (sublimation at 80 °C and 1×10^{-4} mbar), and this caused the relatively low yield.

A series of compounds which incorporate 1,2,4-azadiphosphole rings have previously been synthesized, and the compound N(Ph)P_2C_2ᵗBu$_2$ has been crystallographically characterized.[27] Spectroscopic data for **6** are consistent with the data for these

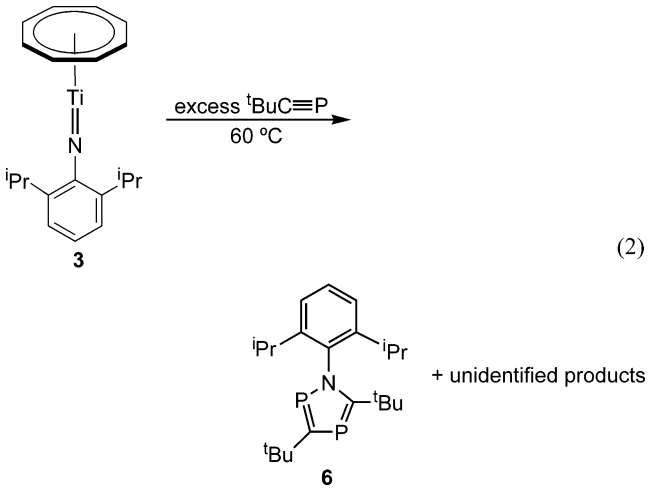

(2)

analogous compounds, and the $^{31}P\{^1H\}$ NMR spectrum of **6** displays the characteristic AX pattern of lines previously observed in other 1,2,4-azadiphosphole rings.[27] The chemical shifts of the two inequivalent phosphorus nuclei are both in the unsaturated region (δ 260.0 and 154.6 ppm, $^2J_{P-P}$ = 29.2 Hz). The low-field resonance is significantly broadened, presumably due to the proximity of the phosphorus nucleus to the quadrupolar ^{14}N nucleus, and the two-bond phosphorus scalar coupling constant is very similar to that reported by Schmidpeter et al. for 1,2,3,5-diazadiphospholes ($^2J_{P-P}$ = 23−25 Hz).[31] Further evidence for the proposed structure is derived from the observation of the quaternary 1,2,4-azadiphosphole ring carbon signals in the $^{13}C\{^1H\}$ NMR spectrum of **6**. These resonances exhibit the expected doublet of doublets splitting for both the PCP and NCP carbon signals.

The experiments described above appear to indicate that there is a difference in the reactivities of the alkylimido species **1** and **2** and the arylimido species **3** with ᵗBuC≡P, and further experiments were consistent with this observation. When reactions of compounds **1** and **2** with 2 equiv of ᵗBuC≡P were performed in an NMR tube at room temperature and monitored by ^{1}H and ^{31}P NMR spectroscopy, the only observed new products were **4** and **5**, respectively, and there was no evidence for any intermediates. These products were formed in quantitative yield after 12 h. In contrast, when the identical reaction between **3** and 2 equiv of ᵗBuC≡P was performed in an NMR tube at room temperature, the only observed new product was **6**, and again there was no evidence for any intermediates. However, the reaction was extremely slow; after 5 days the total yield of **6** was approximately 35% and there were still large amounts of unreacted starting material present. To drive this reaction to completion, it was necessary to heat the reaction mixture, and as a result of the increased volatility of ᵗBuC≡P at higher temperatures, an excess of the phosphaalkyne was required. It should also be noted that identical workup procedures could be used to isolate compounds **4**−**6**, and only the procedures which gave the highest yield are described. Thus, compound **6** could be purified by recrystallization (without sublimation), in a manner similar to that for compounds **4** and **5**, and analogously, compounds **4** and **5** could be purified by sublimation at elevated temperatures (200 °C, 1×10^{-4} mbar for **4** and 220 °C, 1×10^{-4} mbar for **5**). The sublimation of **4** and **5** at elevated temperatures demonstrates that these compounds are thermally stable toward decomposition up to at least

(30) Nugent, W. A.; Mayer, J. M. *Metal−Ligand Multiple Bonds*; Wiley-Interscience: New York, 1988.

(31) Schmidpeter, A.; Leyh, C.; Karaghiosoff, K. *Angew. Chem., Int. Ed. Engl.* **1985**, *24*, 124.

Scheme 1

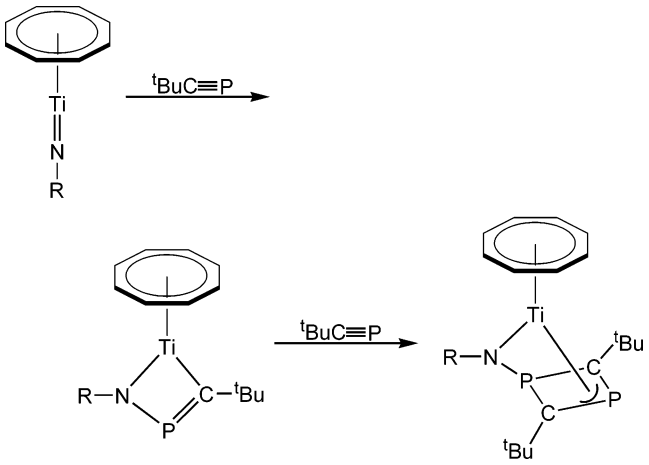

200 °C and it has been mentioned earlier that they are stable in solution at 80 °C even in the presence of excess ^{t}BuC≡P. These observations strongly suggest that the difference in reaction products from compounds **1**−**3** and ^{t}BuC≡P is genuine and is not related to either the reaction conditions or workup procedure.

Despite this experimental study, there are several unanswered questions relating to the reactions of compounds **1**−**3** with ^{t}BuC≡P. First, there is a difference in reactivity between the *tert*-butylimido compounds **1** and **2** and the arylimido species **3**. A difference in reactivity has previously been observed in the reactions of compounds **1** and **3** with isocyanides, but the reasons behind this are unclear.[29] Second, the exact mechanism for the formation of compounds **4**−**6** is also unclear. Although the reactions are assumed to proceed via sequential [2 + 2] cycloadditions of ^{t}BuC≡P with (i) the titanium−nitrogen triple bond and (ii) the resulting P═C double bond (Scheme 1), there is very little direct evidence to support this hypothesis. Presumably, in the reaction between **3** and ^{t}BuC≡P the product of a two-step cycloaddition is unstable and eliminates the organic species **6**. Finally, the structure of compound **4** is quite unusual, and there is uncertainty about the exact bonding of the NC_2P_2 unit. The following sections describe attempts to address these issues using a combination of DFT and PES studies.

DFT Investigation of the Reaction of 1 Equiv of RC≡P with [Ti(NR)(COT)]. We have previously shown that the reaction of the sterically hindered titanium imide [Ti(N^{t}Bu)-{MeC(C_5H_4N-2)(CH_2NSiMe_3)$_2$}(py)] with 1 equiv of ^{t}BuC≡P results in a [2 + 2] cycloaddition and the formation of the stable four-membered metallacycle **A**, which contains Ti−C and P−N bonds.[24] In addition, it has been established that compounds **1**−**3** undergo cycloaddition reactions with substrates that contain multiple bonds, such as CO_2, isocyanates, and isothiocyanates.[29] Therefore, the first step in the reactions of compounds **1**−**3** with ^{t}BuC≡P is proposed to involve a [2 + 2] cycloaddition between 1 equiv of ^{t}BuC≡P and the Ti═N bond of the imide. Experimentally, it was observed that the reaction of **1** or **3** with 1 equiv of ^{t}BuC≡P results in the formation of $^1/_2$ equiv of either **4** or **6**, so the product that is first formed (which was not observed) clearly reacts more quickly with ^{t}BuC≡P than does either **1** or **3**. In theory, a single cycloaddition product could either contain Ti−C and N−P bonds (experimentally observed in other systems[24,26]) or Ti−P and N−C bonds, depending on the orientation of the multiple bond in ^{t}BuC≡P with respect to the Ti═N bond. Thus, to study the reaction of 1 equiv of ^{t}BuC≡P with compounds **1**−**3**, geometry optimizations were performed on the starting materials RC≡P (R = H, Me, ^{i}Pr, ^{t}Bu) and [Ti(NR′)(COT)] (R′ = H, Me, ^{i}Pr, ^{t}Bu, Ar) and also

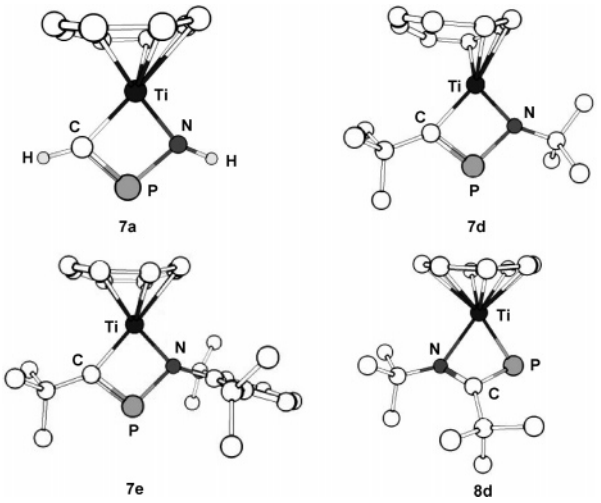

Figure 2. Optimized geometries of [Ti{N(H)PC(H)}(COT)] (**7a**), [Ti{N(^{t}Bu)PC(^{t}Bu)}(COT)] (**7d**), [Ti{N(Ar)PC(^{t}Bu)}(COT)] (**7e**), and [Ti{N(^{t}Bu)C(^{t}Bu)P}(COT)] (**8d**). Selected H atoms are omitted for clarity.

Table 2. Relative SCF Energies[a] of [Ti{N(R′)PC(R)}(COT)] (7a−e) and [Ti{N(R′)C(R)P}(COT)] (8a−e) with Respect to [Ti(NR′)(COT)] and RC≡P

R	R′	Ti−C product **7a**−**e** (kJ mol^{-1})	Ti−P product **8a**−**e** (kJ mol^{-1})
H	H	−49	−97
Me	Me	−9	−63
^{i}Pr	^{i}Pr	0.7	−19
^{t}Bu	^{t}Bu	19	55
^{t}Bu	Ar	28	94

[a] In each case the combined SCF energy of [Ti(NR′)(COT)] and RC≡P is defined as being 0 kJ mol^{-1}.

the hypothetical four-membered metallacycle-containing products [Ti{N(R′)PC(R)}(COT)] (Ti−C products: R = H, R′ = H (**7a**); R = Me, R′ = Me (**7b**); R = ^{i}Pr, R′ = ^{i}Pr (**7c**); R = ^{t}Bu, R′ = ^{t}Bu (**7d**); R = ^{t}Bu, R′ = Ar (**7e**)) and [Ti{N(R′)C-(R)P}(COT)] (Ti−P products: R = H, R′ = H (**8a**); R = Me, R′ = Me (**8b**); R = ^{i}Pr, R′ = ^{i}Pr (**8c**); R = ^{t}Bu, R′ = ^{t}Bu (**8d**); R = ^{t}Bu, R′ = Ar (**8e**)). No symmetry constraints were used in any of the optimizations. Fragment analyses were performed on all complexes of the type [Ti{N(R′)PC(R)}(COT)] (**7a**−**e**) and [Ti{N(R′)C(R)P}(COT)] (**8a**−**e**), in which the molecules were separated into Ti(COT) and either {N(R′)PC(R)} or {N-(R′)C(R)P} fragments, respectively. The optimized geometries of [Ti{N(H)PC(H)}(COT)] (**7a**), [Ti{N(^{t}Bu)PC(^{t}Bu)}(COT)] (**7d**), [Ti{N(Ar)PC(^{t}Bu)}(COT)] (**7e**), and [Ti{N(^{t}Bu)C(^{t}Bu)P}-(COT)] (**8d**) are shown in Figure 2, and Table 2 gives the relative SCF energies of the products [Ti{N(R′)PC(R)}(COT)] (**7a**−**e**) and [Ti{N(R′)C(R)P}(COT)] (**8a**−**e**) with respect to the appropriate starting materials ([Ti(NR′)(COT)] and RC≡P).

The optimized structures of the family of compounds [Ti-{N(R′)PC(R)}(COT)] (**7a**−**e**) reveal that there is little change in the bonding of the {N(R′)PC(R)} fragment to the titanium center as the steric bulks of both the N substituent and C substituent are varied. In all cases the four-membered metallacyclic rings are planar, with the Ti−C bond distances ranging from 2.08 to 2.12 Å and the Ti−N distances ranging from 1.83 to 1.86 Å. These Ti−N distances are longer than those observed in the starting imido compounds [Ti(N^{t}Bu)(COT)] (**1**) and [Ti-(NAr)(COT)] (**3**) (Ti−N = 1.699(6) Å in **1** and Ti−N = 1.7217-(18) Å in **3**)[28] and indicate that on formation of the metallacyclic ring there is a decrease in the Ti−N bond order. Similarly, the C−P bond distances in the optimized structures of compounds

7a−**e** range from 1.68 to 1.70 Å and are considerably longer than the C−P distances in the optimized structures of RC≡P (C≡P distances range from 1.55 to 1.56 Å). The Ti−P distances vary from 2.59 to 2.67 Å, which suggests that there could be an interaction between the metal center and the phosphorus atom. However, analysis of the molecular orbitals indicates that there is no clear bonding interaction between the two atoms. Overall, the bonding of the {N(R′)PC(R)} fragment to the titanium center in compounds **7a**−**e** appears to be similar to that observed in the crystallographically characterized species [Ti{N(ᵗBu)PC(ᵗBu)}{MeC(C_5H_4N-2)(CH_2NSiMe_3)$_2$}].[24]

One of the most interesting features of the optimized structures of compounds **7a**−**e** is the bonding of the COT ring to the Ti center. In all five compounds the COT ligand is distorted from planarity and the ring forms a saddle shape. The Ti−C distances are variable, with the longest distances being those trans to the Ti−N bonds. The C−C distances in the COT ring vary, and the carbon atoms which are further away from the Ti center tend to form shorter C−C bonds. The extent of this distortion is similar in compounds **7a**−**c**,**e**, with Ti−C distances varying from 2.28 to 2.75 Å and six carbon atoms of the COT ring being within 2.50 Å of the metal center and the other two atoms of the ring being within 2.75 Å. This distortion of the COT ring in **7a**,**e** is clearly shown in Figure 2. In compound **7d**, which has *tert*-butyl substituents on both the nitrogen and carbon atoms of the metallacycle, the distortion of the COT ring is significantly greater than in compounds **7a**−**c**,**e**. The two carbon atoms of the COT ring which are directly opposite the Ti−N bond are 3.16 Å away from the metal center, and the distance between the titanium atom and the other two carbon atoms opposite the Ti−N bond is 2.74 Å. The COT ring can be considered to be coordinating to the metal center in an η^6 fashion, but molecular orbital analysis indicates that it is still acting as a dianionic ligand (no electrons are localized on Ti, indicating that the formal oxidation state of Ti is still +4). This is not unexpected, as previous studies have shown that the COT ligand can act as a dianionic ligand even when it is not η^8 coordinated.[32] At this stage the exact reasons why ring slippage occurs in **7d** and not in **7a**−**c**,**e** are unknown, although it is well established that *tert*-butylimido substituents have a greater trans influence than other N substituents[33] and that the energy gap between two different conformations of the COT ligand can often be small.[32]

In contrast to the series of complexes **7a**−**e**, there are only small changes in the optimized geometries of complexes of the type [Ti{N(R′)C(R)P}(COT)] (**8a**−**e**) as the steric bulk on both the nitrogen and carbon substituents of the metallacycle is varied. The COT ring is η^8-coordinated in all cases, although there is a slight disparity in the Ti−N distances due to the trans influence of the nitrogen donor atom being different from that of the phosphorus donor atom. The average Ti−C distance increases as the N substituent becomes larger, and this probably reduces any unfavorable steric interactions between the N substituent and the COT ring. The most striking features of the bonding in compounds **8a**−**e** are the extremely short N−C bond lengths (N−C bond distances range from 1.31 to 1.33 Å), and this is presumably a driving force in the formation of products with a Ti−P bond. The short N−C bond lengths result in longer C−P and Ti−N bond lengths (C−P bond lengths range from 1.78 to 1.85 Å and Ti−N bond lengths range from 2.13 to 2.29 Å) as compared to those observed for compounds **7a**−**e**. There is a large variation in the Ti−N bond lengths, with the shortest bond length being observed in **8a** (Ti−N is 2.13 Å) and the longest in **8d** (Ti−N is 2.23 Å) and **8e** (Ti−N is 2.29 Å). This increase in the Ti−N bond distance as the steric bulk on the N and C substituents is increased may help to relieve steric strain between the substituents of the {N(R′)C(R)P} fragment. It is almost certainly more energetically favorable to lengthen the Ti−N bond than to lengthen the extremely strong C−N bond.

The relative SCF energies of compounds **7a**−**e** and **8a**−**e** in Table 2 indicate that as the sizes of the N and C substituents are increased, it becomes more favorable to form products with a Ti−C rather than a Ti−P bond. Thus, compounds **8a**−**c** are more stable than compounds **7a**−**c**, but compounds **7d**,**e** are more stable than compounds **8d**,**e**. Presumably when the N and C substituents are small, the Ti−P product is favored because an extremely strong C−N multiple bond is being formed. However, it was noted earlier that as the steric bulk on the N and C substituents is increased, the Ti−N bonds in compounds **8a**−**e** lengthen. In contrast, as the steric bulk on the N and C substituents in compounds **7a**−**e** is increased, the only major change is the bonding of the COT ring to the metal center, and this has been shown to only have a small effect on the overall energy of the molecule.[32] Thus, it appears that the energy loss from lengthening the Ti−N bond in compounds **8d**,**e** is sufficiently large that it becomes more favorable to form compounds **7d**,**e** with a Ti−C bond. This is consistent with experimental results, which indicate that Ti−C products are preferred, and reveals that steric considerations are important in modeling this system. Overall, SCF energies indicate that the reactions to form **7d**,**e** from ᵗBuC≡P and **1** and **3**, respectively, are slightly energetically unfavorable (18.55 kJ mol^{-1} for **7d** and 27.70 kJ mol^{-1} for **7e**) but this is not significant, given that **7d**,**e** are only being postulated as intermediates.

The formation of compounds **7a**−**e** from [Ti(NR)(COT)] and RC≡P can be explained by considering the frontier orbitals of the starting materials. The HOMO in compounds **7a**−**e** represents a π-bond between one of the nitrogen 2p orbitals and a metal orbital of suitable symmetry (polarized so that there is more electron density on the nitrogen atom), while the LUMO is essentially a $3d_{z^2}$ orbital. The frontier orbitals of RC≡P are similar to those of CO_2,[34,35] with the HOMO representing a C−P π-bonding orbital (polarized so that there is more electron density on the carbon atom) and the LUMO representing a C−P π*-antibonding orbital (polarized so that it is more localized on the phosphorus atom). Thus, the frontier orbitals of [Ti(NR)(COT)] are ideally matched for interaction with both the HOMO and LUMO of RC≡P, in a manner that will eventually generate both Ti−C and N−P bonds. Figure 3 shows the HOMO and LUMO of [Ti(NᵗBu)(COT)] (**1**) and ᵗBuC≡P.

The transition states for the addition of [Ti(NᵗBu)(COT)] (**1**) and ᵗBuC≡P and [Ti(NAr)(COT)] (**3**) and ᵗBuC≡P to form **7d**,**e**, respectively, are shown in Figure 4, along with the relative SCF energies of the transition states compared with those of the starting materials (the transition states are labeled $\mathbf{7d_{TS}}$ and $\mathbf{7e_{TS}}$). The formation of the Ti−C and N−P bonds was found to occur simultaneously via a [2 + 2] cycloaddition. In both cases the multiple bond of ᵗBuC≡P does not approach the Ti−N π-bond in a perfectly side-on fashion, but instead the Ti−N−P−C dihedral angle is 42.1° in $\mathbf{7d_{TS}}$ and 37.1° in $\mathbf{7e_{TS}}$. This is in contrast to [2 + 2] cycloaddition reactions between CO_2 and

(32) Cloke, F. G. N.; Green, J. C.; Hitchcock, P. B.; Joseph, S. C. P.; Mountford, P.; Kaltsoyannis, N.; McCamley, A. *J. Chem. Soc., Dalton Trans.* **1994**, 2867.

(33) Kaltsoyannis, N.; Mountford, P. *J. Chem. Soc., Dalton Trans.* **1999**, 781.

(34) Jalbout, A. F. *Int. J. Quantum Chem.* **2002**, *86*, 541.

(35) Jayasuriya, K. *Int. J. Quantum Chem.* **1992**, *44*, 327.

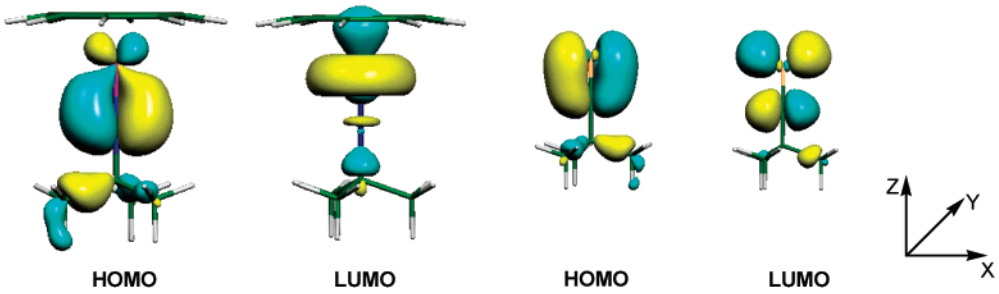

Figure 3. HOMO and LUMO of [Ti(NᵗBu)(COT)] (**1**)[28] and ᵗBuC≡P.

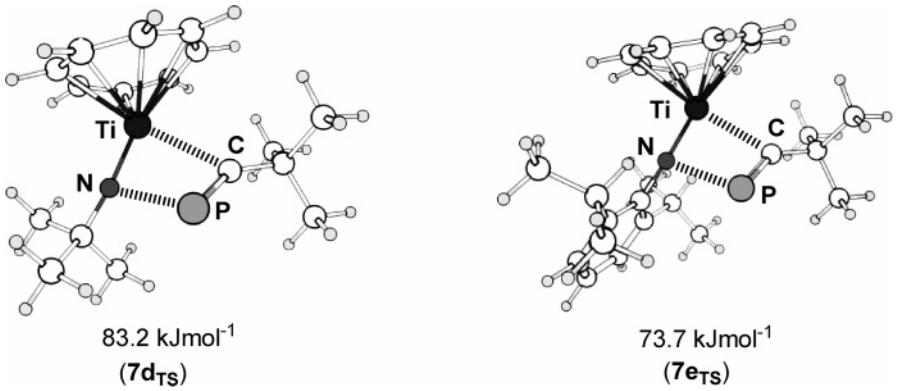

Figure 4. Optimized geometries of $\mathbf{7d_{TS}}$ and $\mathbf{7e_{TS}}$ and relative SCF energies (compared with starting materials) of $\mathbf{I_{dTS}}$ and $\mathbf{I_{eTS}}$.

titanium imides, where it has been shown that the CO_2 approaches the Ti−N π-bond in a perfectly side-on fashion and the Ti−N−C−O bond dihedral angle is 0°.[36] In this case it is sterically unfavorable for the phosphaalkyne to approach the imide in a side-on fashion, as this would result in a clash between the COT ring and the *tert*-butyl substituent of ᵗBuC≡P. The barrier (SCF energy) for the formation of **7d** from **1** and ᵗBuC≡P is 83.2 kJ mol^{-1}, while the barrier for the formation of **7e** from **3** and ᵗBuC≡P is 73.7 kJ mol^{-1}. The slightly higher barrier for cycloaddition to the alkylimido complex **1** probably relates to the fact that the Ti=NᵗBu bond is stronger than the Ti=NAr bond.[28] Both of these calculated barriers are much higher than the calculated barrier for the reaction of the model compound [Ti(η^5-C_5H_5)(NMe){MeC(NMe)$_2$}] with CO_2 (the electronic barrier is 0.6 kJ mol^{-1}), but this is probably attributable to the increased steric bulk of ᵗBuC≡P compared with that of CO_2.

The results in this section clearly demonstrate that compounds **7d**,**e** are possible intermediates in the reactions of compounds **1** and **3** with ᵗBuC≡P. Although other mechanisms cannot be ruled out from these calculations, an initial [2 + 2] cycloaddition of a single molecule of ᵗBuC≡P with **1** or **3** is energetically plausible, and a simple pathway exists from compounds **1** and **3** and ᵗBuC≡P to compounds **7d**,**e**, respectively. In addition, there are numerous experimental examples of [2 + 2] cycloadditions between titanium imides and organic substrates containing a multiple bond[6] and [2 + 2] cycloadditions have previously been proposed as the first step in reactions between other transition-metal complexes and RC≡P (although often with little direct evidence).[23,37,38]

DFT Investigation of the Reaction of a Second Equivalent of RC≡P with [Ti{N(R)PC(R)}(COT)]. Previously, it has been postulated that the mechanism for the formation of 1,3,5-triphosphabenzenes from [V(NᵗBu)$_3$Cl$_3$] and RC≡P (R = ᵗBu, CMe_2Et, 1-adamantyl, 1-methylcyclopentyl or 1-methylcyclohexyl) involves an initial [2 + 2] cycloaddition of RC≡P to [V(NᵗBu)$_3$Cl$_3$], which generates a four-membered metallacycle with a V−C bond.[23] This is followed by the insertion of another molecule of RC≡P into the *vanadium−carbon* bond of the metallacycle. Similarly, the mechanism for the formation of azatetraphosphaquadricyclanes from [V(NᵗBu)Cl$_3$(DME)] and RC≡P (R = ᵗBu, CMe_2Et, 1-adamantyl, 1-methylcyclopentyl or 1-methylcyclohexyl) is also believed to involve an initial [2 + 2] cycloaddition of RC≡P to [V(NᵗBu)$_3$Cl$_3$(DME)], which generates a four-membered metallacycle with a V−C bond.[37] However, in contrast to the reaction between [V(NᵗBu)$_3$Cl$_3$] and RC≡P, this is followed by the insertion of a second molecule of RC≡P into the *vanadium−nitrogen* bond of the metallacycle. The previous section demonstrated that the formation of **4** from ᵗBuC≡P and **1** probably proceeds via an initial [2 + 2] cycloaddition to generate **7d**. Subsequently, a second molecule of ᵗBuC≡P could insert into the Ti−C bond of compound **7d** to form the unsymmetrical product [Ti{N(ᵗBu)PC(ᵗBu)PC(ᵗBu)}(COT)] (**4a**), which contains both Ti−C and Ti−N bonds (Scheme 2). Compound **4a** could then isomerize to give the observed experimental product **4**; however, the direct conversion of **7d** to **4** is also possible. Unfortunately, due to the large size of the molecules being studied, repeated attempts to find transition states for the conversion of **7d** to **4** were unsuccessful (it should be noted that work in the previous section and another recent computational study investigating organic reactions of ᵗBuC≡P[39] indicate that steric considerations are important and thus simplified model compounds could not be used). Nevertheless, the stabilities and bonding in compounds **4** and **4a** and also the symmetric compound [Ti{C(ᵗBu)PN(ᵗBu)PC(ᵗBu)}(COT)] (**4b**) (which would arise from the insertion of a molecule of ᵗBuC≡P into the Ti−N bond of **7d** and is shown in Scheme

(36) Boyd, C. L.; Clot, E.; Guiducci, A. E.; Mountford, P. *Organometallics* **2005**, *24*, 2347.

(37) Peters, C.; Tabellion, F.; Nachbauer, A.; Fischbeck, U.; Preuss, F.; Regitz, M. *Z. Naturforsch., C: Biosci.* **2001**, *56*, 951.

(38) Jamison, G. M.; Wheeler, D. R.; Loy, D. A.; Ziller, J. W. *Organometallics* **2005**, *24*, 2245.

(39) Nyulaszi, L. *J. Organomet. Chem.* **2005**, *690*, 2597.

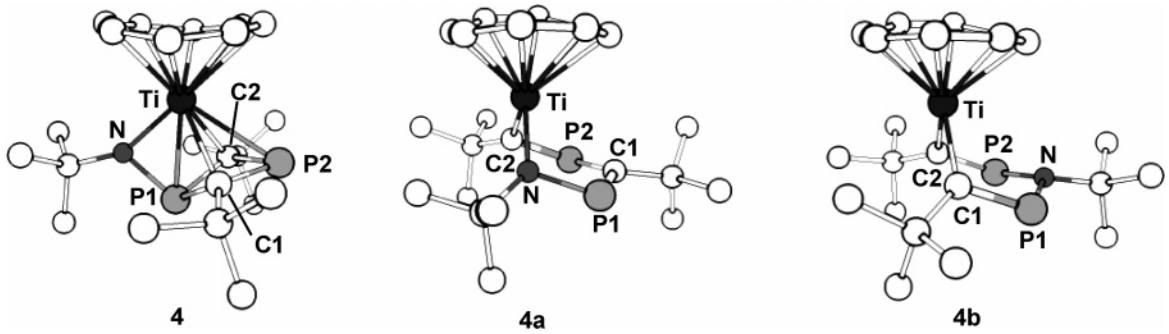

Figure 5. Optimized geometries of [Ti{N(ᵗBu)PC(ᵗBu)PC(ᵗBu}(COT)] (**4** or **4a**) and [Ti{C(ᵗBu)PN(ᵗBu)PC(ᵗBu)}(COT)] (**4b**). H atoms are omitted for clarity.

Scheme 2

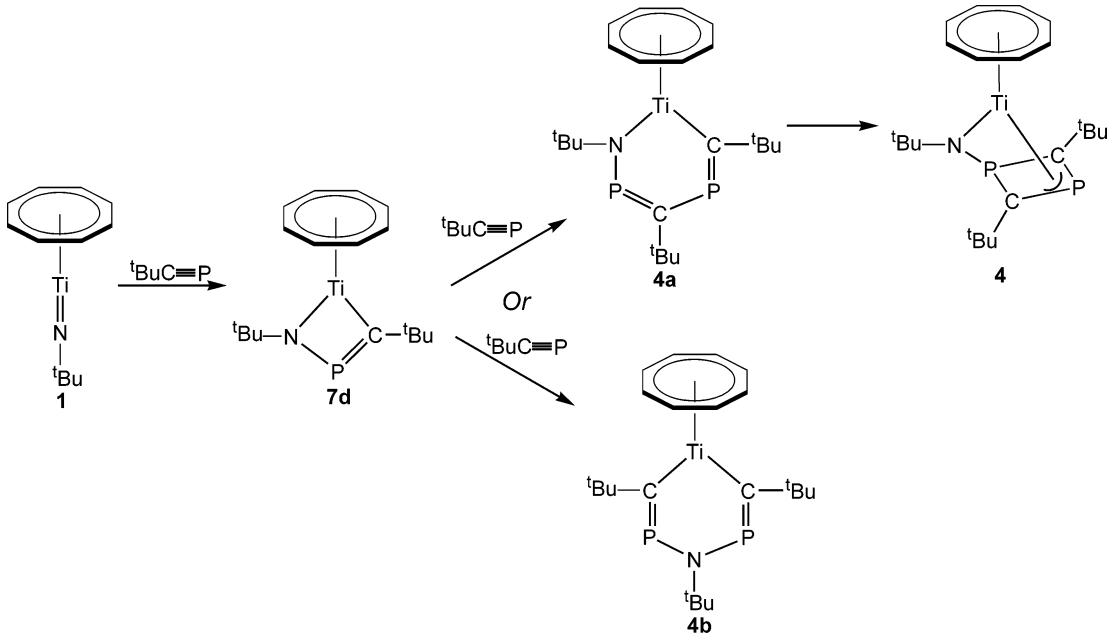

2) can be compared and the reasons for the formation of **4** under thermodynamic conditions established.

Geometry optimizations were performed on compounds **4** and **4a**,**b** and also on an analogous series of compounds with a 2,6-$^{i}Pr_2C_6H_3$ substituent on the nitrogen atom ([Ti{N(Ar)PC(ᵗBu)PC(ᵗBu)}(COT)] (**9**) analogous to **4**, [Ti{N(Ar)PC(ᵗBu)PC(ᵗBu)}(COT)] (**9a**) analogous to **4a**, and [Ti{C(ᵗBu)PN(Ar)PC(ᵗBu)}(COT)]) (**9b**) analogous to **4b**). No symmetry constraints were used in any of the optimizations. Fragment analyses were performed on complexes **4** and **4a**,**b** and on **9** and **9a**,**b** in which the molecules were separated into Ti(COT) and either {N(ᵗBu)PC(ᵗBu)PC(ᵗBu)} or {C(ᵗBu)PN(ᵗBu)PC(ᵗBu)} fragments, respectively. Important calculated bond lengths and angles in **4** are compared with the experimental values in Table 1. The optimized geometries of **4** and **4a**,**b** are shown in Figure 5, and Table 3 gives the relative SCF energies of the products **4** and **4a**,**b** and **9** and **9a**,**b** with respect to the appropriate starting materials ([Ti(NR)(COT)] and 2 equiv of ᵗBuC≡P). In Table 4 the Mulliken overlap population and relative binding energies between the {N(ᵗBu)PC(ᵗBu)PC(ᵗBu)} or {C(ᵗBu)PN(ᵗBu)PC(ᵗBu)} fragments and the Ti(COT) fragments in compounds **4** and **4a**,**b** and the Hirshfeld[40,41] charge on the {N(ᵗBu)PC(ᵗBu)PC(ᵗBu)} or {C(ᵗBu)PN(ᵗBu)PC(ᵗBu)} fragments are given. (In Table 4 the binding energy of the {N(ᵗBu)PC(ᵗBu)PC(ᵗBu)} fragment in **4** is defined as being 0 kJ mol^{-1} and all other binding energies are given relative to this value.)

Table 3. Relative SCF Energies[a] of [Ti{N(R)PC(ᵗBu)PC(ᵗBu)}(COT)] (R = ᵗBu (4 and 4a), Ar (9 and 9a)) and [Ti{C(ᵗBu)PN(R)PC(ᵗBu)}(COT)] (R = ᵗBu (4b), Ar (9b)) with Respect to [Ti(NR)(COT)] and 2 ᵗBuC≡P

compd	energy (kJ mol^{-1})	compd	energy (kJ mol^{-1})
4	−29	**9**	−68
4a	12	**9a**	−14
4b	87	**9b**	73

[a] In each case the combined SCF energy of [Ti(NR′)(COT)] and 2 equiv of ᵗBuC≡P is defined as being 0 kJ mol^{-1}.

It can be seen from Table 1 that calculated bond lengths and angles for **4** show good agreement with the experimental values, providing strong evidence that the computational approach is valid. Given that the structure of **4** has been discussed above, it will not be described further here. Interestingly, in the structure of **4a** the Ti−N bond length is only slightly shorter than the Ti−C(1) bond length (Ti−N = 2.00 Å and Ti−C(1) = 2.02 Å), despite the different donor properties of nitrogen and carbon. The N−P(1) and C(1)−P(2) bond distances are also similar (N−P(1) = 1.72 Å and Ti−C(1) = 1.73 Å), but the C−P bond lengths are different (C(2)−P(1) = 1.74 Å and C(2)−P(2) = 1.82 Å). The six-membered metallacyclic ring formed by Ti−N−P(1)−C(2)−P(2)−C(1) is nonplanar, with the Ti atom lying well above the plane containing N, P(1), P(2), and C(2) (these

(40) Hirshfeld, F. L. *Theor. Chim. Acta* **1977**, *44*, 129.
(41) Wiberg, K. B.; Rablen, P. R. *J. Comput. Chem.* **1993**, *14*, 1504.

Table 4. Hirshfeld[40,41] Charges on {N(^{t}Bu)PC(^{t}Bu)PC(^{t}Bu)} or {C(^{t}Bu)PN(^{t}Bu)PC(^{t}Bu)} Fragments in 4 and 4a,b and Mulliken Overlap Populations and Relative Binding Energies[a] between {N(^{t}Bu)PC(^{t}Bu)PC(^{t}Bu)} or {C(^{t}Bu)PN(^{t}Bu)PC(^{t}Bu)} and Ti(COT) Fragments in 4 and 4a,b

compd	fragment	charge	overlap pop.	binding energy (kJ mol^{-1})
4	{N(^{t}Bu)PC(^{t}Bu)PC(^{t}Bu)}	−0.014	0.14	0
4a	{N(^{t}Bu)PC(^{t}Bu)PC(^{t}Bu)}	−0.067	0.11	13
4b	{C(^{t}Bu)PN(^{t}Bu)PC(^{t}Bu)}	−0.064	0.058	86

[a] The binding energy of the {N(^{t}Bu)PC(^{t}Bu)PC(^{t}Bu)} fragment to the Ti(COT) fragment in **4** is defined as being 0 kJ mol^{-1}.

four atoms are coplanar) and C(1) also positioned slightly out of this plane. This distortion from planarity is presumably for steric reasons, as a planar six-membered metallacyclic ring would result in unfavorable interactions between the *tert*-butyl substituents of the ring. Indeed, when the *tert*-butyl substituents in **4a** were replaced with H substituents, the compound was optimized to a structure which contained a planar six-membered metallacyclic ring that was perpendicular to the COT ring. The COT ring in **4a** is η^8-coordinated, although differences are observed in the Ti−C bond lengths as a result of the trans influence of the nitrogen donor atom being different from that of the carbon donor atom.

The structure of **4b** is similar to that of **4a** and is almost completely C_s symmetrical. The Ti−C(1) bond length is 2.08 Å, and the Ti−C(2) bond length is 2.09 Å, which indicate that the shorter Ti−C(1) bond in **4a** (Ti−C(1) = 2.02 Å) is stronger than either of the Ti−C bonds in **4b**. The C−P bond distances in **4b** (C(1)−P(1) and C(2)−P(2) = 1.72 Å) are shorter than those in **4a**, demonstrating that the two molecules of ^{t}BuC≡P incorporated in **4b** are less activated than those in **4a**. The long Ti−N distance of 3.17 Å indicates that there is no covalent interaction between these two atoms. Once again, the six-membered metallacycle is nonplanar and this is probably due to steric considerations. The structures of the TiN(Ar)C_2(^{t}Bu)$_2P_2$ cores in compounds **9** and **9a**,**b** are almost identical with those in the corresponding compounds **4** and **4a**,**b**. In compounds **9** and **9a** the aryl ring on the N substituent lies approximately parallel with the COT ring, while in compound **9b** the aryl ring is positioned perpendicular to the COT ring in order to minimize steric interactions between the isopropyl substituents on the aryl ring and the metallacycle (see the Supporting Information for the optimized structures of **9** and **9a**,**b**).

The relative SCF energies of compounds **4** and **4a**,**b** clearly indicate that compound **4** is the most stable and compound **4b** the least stable. A similar pattern is observed for compounds **9** and **9a**,**b**. The stability of compounds **4** and **4a**,**b** can be directly related to the donor properties of the {N(^{t}Bu)PC(^{t}Bu)PC(^{t}Bu)} or {C(^{t}Bu)PN(^{t}Bu)PC(^{t}Bu)} fragments. In compound **4a** only the N atom and C(2) of the {N(^{t}Bu)PC(^{t}Bu)PC(^{t}Bu)} fragment interact with the Ti center, whereas in **4** the N atom, C(1), C(2), and P(2) of the {N(^{t}Bu)PC(^{t}Bu)PC(^{t}Bu)} fragment all interact with the Ti center (see below for a full description of the bonding in **4**). As a result, the Mulliken overlap population between the {N(^{t}Bu)PC(^{t}Bu)PC(^{t}Bu)} and the Ti(COT) fragments in **4** is greater than in **4a** (Table 4) and the Hirshfeld charge on the {N(^{t}Bu)PC(^{t}Bu)PC(^{t}Bu)} fragment in **4** is significantly lower than in **4a**. Similarly, Table 4 also shows that the Mulliken overlap population between the {N(^{t}Bu)PC(^{t}Bu)PC(^{t}Bu)} and Ti(COT) fragments in **4a** is much larger than the overlap between the {C(^{t}Bu)PN(^{t}Bu)PC(^{t}Bu)} and Ti(COT) fragments in **4b**. This is presumably related to the fact that N is a much better donor to Ti than is C and that the single Ti−C bond distance in **4a** is shorter than both Ti−C bond distances in **4b**. Thus, the {N(^{t}Bu)PC(^{t}Bu)PC(^{t}Bu)} fragment in **4** is better at stabilizing the Ti(COT) fragment than is the {N(^{t}Bu)PC(^{t}Bu)-PC(^{t}Bu)} fragment in **4a**, and in turn the Ti(COT) fragment is better stabilized by the unsymmetrical {N(^{t}Bu)PC(^{t}Bu)PC(^{t}Bu)} fragment in **4a** than by the symmetric {C(^{t}Bu)PN(^{t}Bu)PC(^{t}Bu)} fragment in **4b**. The relative abilities of the three NC_2P_2 fragments to stabilize the Ti(COT) fragment are also supported by the relative binding energies of the NC_2P_2 fragments to the Ti(COT) fragment (as shown in Table 4), and this is probably a key factor in determining the relative energies of compounds **4** and **4a**,**b**.

Table 5. Experimental and Calculated ^{13}C and ^{31}P NMR Chemical Shifts for [Ti(N(^{t}Bu)PC(^{t}Bu)PC(^{t}Bu))(COT)] (4)[a]

	exptl (ppm)	calcd (ppm)
NPC*P*C, P(1)	−190.8	−190
N*P*CPC, P(2)	215.1	227
PCCCH$_3$, C(1) and C(2)[b]	185.3	197
COT, C(15)−C(22)[b]	96.3	98
NC(CH$_3$)$_3$, C(11)	61.2	66
PC*C*(CH$_3$)$_3$, C(3) and C(11)[b]	39.3	45
PCC(*C*H$_3$)$_3$[b]	34.7	32
NC(*C*H$_3$)$_3$[b]	34.3	36

[a] Chemical shifts referenced to TMS at 0 ppm for ^{13}C and neat H_3PO_4 at 0 ppm for ^{31}P. [b] Calculated values represent the average of the carbon environments.

Arguments similar to those made above can be used to rationalize the relative energies of compounds **9** and **9a**,**b**. Overall, it is energetically favorable to form **4** or **9** from 2 equiv of ^{t}BuC≡P and [Ti(N^{t}Bu)(COT)] (**1**) or [Ti(NAr)(COT)] (**3**), respectively. When the relative energies of compounds **4** and **9** and the single cycloaddition products **7d**,**e** with respect to the appropriate starting materials (Tables 2 and 3) are compared, it can be seen that it is more energetically favorable to react **1** or **3** with 2 equiv of ^{t}BuC≡P. This is consistent with experimental observations that the reaction of **1** or **3** with 1 equiv of ^{t}BuC≡P results in the formation of $^1/_2$ equiv of either **4** or **6**.

DFT Analysis of the Bonding in [Ti{N(^{t}Bu)PC(^{t}Bu)PC(^{t}Bu)}(COT)] (4). It has been noted earlier that the structure of [Ti{N(^{t}Bu)PC(^{t}Bu)PC(^{t}Bu)}(COT)] (**4**) is quite unusual and that the exact bonding of the NC_2P_2 unit to the metal center is unclear. The previous section established that it is energetically more favorable to form **4** from **7d** and ^{t}BuC≡P than either **4a** or **4b**. In this section a more complete description of the bonding in **4** is presented, using the geometry optimization and fragment analysis from the previous section. In addition, the ^{13}C and ^{31}P NMR chemical shifts were calculated for the model compound and are compared with the experimental values in Table 5.

It can be seen from Table 5 that the calculated ^{13}C and ^{31}P NMR chemical shifts for **4** show good agreement with the experimental values, providing further evidence that the method is valid. The fragment analysis shows that the σ- and π-symmetry orbitals of the COT ring are too low in energy to interact with the metal center and that they do not mix with any orbitals of the NC_2P_2 fragment (symmetry labels are with respect to the metal ring axis; σ is equivalent to π_1, and π is equivalent to π_2 and π_3 in the standard description of bonding in carbocycles[42]). In contrast, there is a significant amount of mixing between the δ-symmetry orbitals (equivalent to π_4 and π_5) of the COT ring, the Ti center, and the frontier orbitals of the NC_2P_2 fragment, as shown by the representations of the HOMO-5, HOMO-4, HOMO-3, HOMO-1, and HOMO in Figure 6. This

(42) Elian, M.; Chen, M. M. L.; Mingos, D. M. P.; Hoffmann, R. *Inorg. Chem.* **1976**, *15*, 1148.

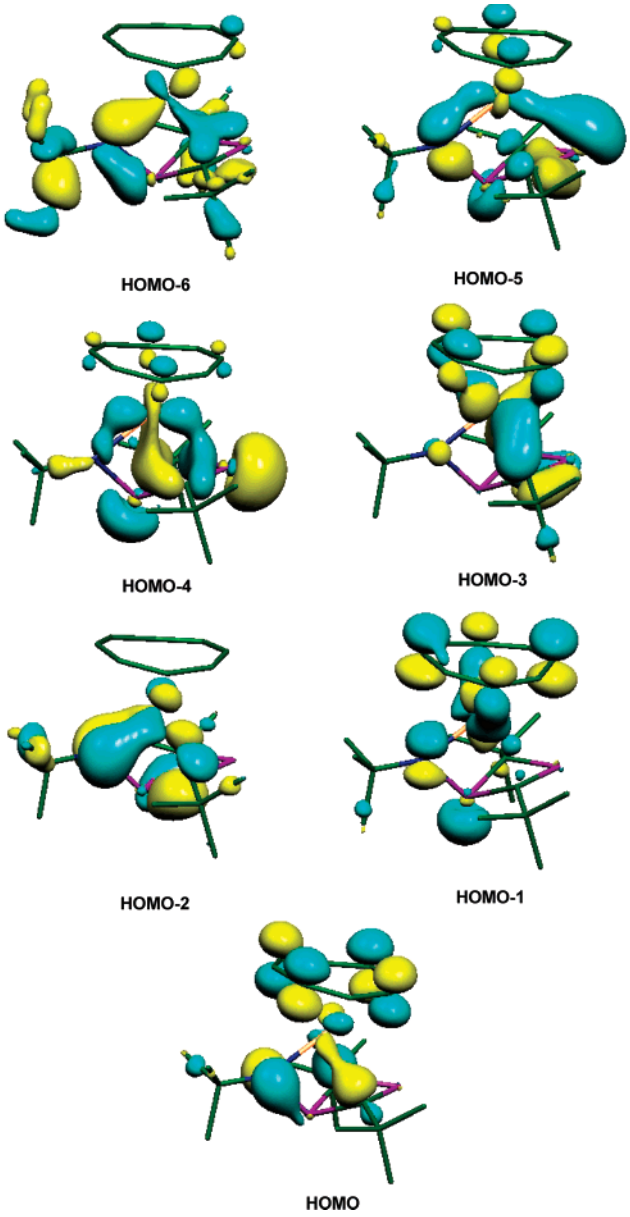

Figure 6. Representations of selected MOs of [Ti{N(ᵗBu)PC(ᵗBu)-PC(ᵗBu)}(COT)] (**4**). H atoms are omitted for clarity.

results in a net decrease in the overlap between the titanium center and the COT ring in compound **4** compared to that in [Ti(NᵗBu)(COT)] (**1**) and, along with the increased coordination number around the metal center, probably explains why there is a significant increase in the Ti−COT ring centroid distance in **4** compared with that in **1**.[28]

The bonding of the NC_2P_2 fragment to the metal center is noteworthy for several reasons. First, the HOMO-5 shows that P(2) donates a lone pair of electrons to the metal center, while conversely the HOMO-1 and HOMO-4 show that P(1) does not and that the lone pair is localized on the phosphorus atom. In addition, the HOMO-6 indicates that there is some delocalization of electron density among atoms C(1), P(2), and C(2). This is consistent with both the calculated and experimental ^{31}P NMR data, which suggest that P(2) is electron-deficient (exptl δ(P(2)) 215.4 ppm) and that P(1) is electron-rich (exptl δ(P(1)) −190.8 ppm). The HOMO-4 shows that C(1) and C(2) bond directly to the metal center in a σ-fashion, and it appears that C(1) and C(2) are in identical electronic environments. This is again consistent with both the experimental and calculated ^{13}C NMR data, in which only one resonance is observed/ predicted for C(1) and C(2). In contrast to the case for [Ti(NᵗBu)(COT)] (**1**), where the N atom of the imide forms two π-bonds with the metal center, the N atom of the NC_2P_2 fragment in **4** forms only a single π-bond with the titanium (HOMO-2), which is consistent with the longer Ti−N bond observed in **4** compared with that in **1**.[28] Finally, it should be noted that the HOMO of **4** is almost entirely ligand-based and has very little metal character.

The interaction of the NC_2P_2 fragment with the metal center can be summarized in the following way. Both C atoms of the C_2P_2 ring form a bond with the Ti center, as does P(2), and there is also some delocalization of electron density among these three atoms. In contrast, the lone pair on P(1) is localized on the phosphorus nucleus and P(1) does not donate to the metal center. The N atom of the NC_2P_2 unit forms a σ-bond with P(1) and also one σ- and one π-bond with the metal center. Overall, the apparent total valence electron count of the complex is 20 electrons: 8 from the COT ligand, 8 from the NC_2P_2 fragment and 4 from the metal center. However, the HOMO is almost entirely ligand-based and the contribution from the Ti center to the HOMO is less than 5%.

Photoelectron Spectra of [Ti{N(ᵗBu)PC(ᵗBu)PC(ᵗBu)}-(COT)] (4). The gas-phase He I and He II photoelectron (PE) spectra of [Ti{N(ᵗBu)PC(ᵗBu)PC(ᵗBu)}(COT)] (**4**) are shown in Figure 7, and vertical ionization energies (IEs) and relative band intensities are summarized in Table 6. The PES bands were assigned by comparison between both experimental and calculated ionization energies and also by comparison between the spectra of **4** and those of other related cyclooctatetraenyl complexes.[28] The calculated IEs and the assignment of PES bands are also given in Table 6, while representations of the orbitals responsible for selected ionizations are given in Figure 6.

In general, good agreement was observed between calculated and experimental ionization energies. Six ionizations are calculated to occur in the region between 6.32 and 8.10 eV. The seventh ionization is estimated to have an IE of 9.09 eV, resulting in a gap of almost 1 eV between the bands predicted for the HOMO-5 and HOMO-6 of **4**. Thus, bands A−D (which occur between 6.46 and 8.40 eV) need to accommodate six ionization processes. From the relative band intensities it is most probable that band C consists of three ionizations and that bands A−C all consist of a single ionization. Band A at 6.46 eV can be assigned to ionization from the HOMO of complex **4** and shows diminished relative intensity in the He II spectrum. Band B corresponds to ionization from the HOMO-1 of **4**, which is primarily a Ti−COT ring δ-bonding orbital. In the PE spectrum of [Ti(NᵗBu)(COT)] (**1**), ionization from the Ti−COT ring δ-bonding orbitals occurs at approximately 8 eV,[28] whereas in **4** this ionization is observed at 6.93 eV. This decrease in the ionization energy is consistent with a decrease in the overlap between the metal center and the COT ring δ-bonding orbitals in **4** compared with that in **1**. It appears that ionizations from the HOMO-2, HOMO-3, and HOMO-4 of **4** all overlap, resulting in the complicated structure that is observed for band C. Band D at 8.40 eV is assigned to ionization from the HOMO-5 of **4**, which consists primarily of phosphorus character (Figure 6). It shows a diminished relative intensity in the He II spectrum and similar characteristics have been observed from ion states associated with the phosphorus atom of the phospholyl ring in [NiCp*(2,5-ᵗBu$_2$PC$_4$H$_2$)] (IE = 8.94 eV)[43] and also

(43) Burney, C.; Carmichael, D.; Forissier, K.; Green, J. C.; Mathey, F.; Ricard, L. *Chem. Eur. J.* **2005**, *11*, 5381.

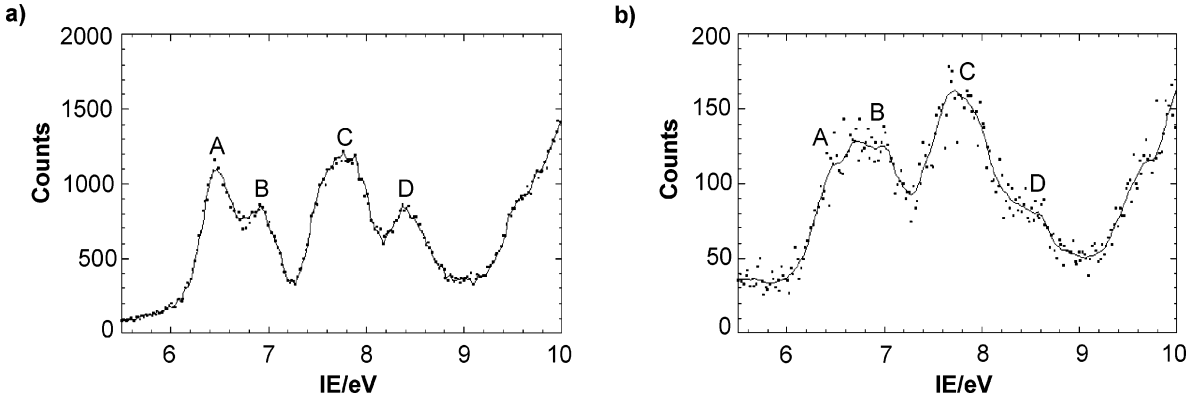

Figure 7. He I (a) and He II (b) spectra for [Ti{N(ᵗBu)PC(ᵗBu)PC(ᵗBu)}(COT)] (**4**).

Table 6. Experimental and Calculated IEs for [Ti{N(ᵗBu)PC(ᵗBu)PC(ᵗBu)}(COT)] (4) and Assignment of PES Bands

		intensity[a]			
band	exptl IE (eV)	He I	He II	assign	calcd IE (eV)
A	6.46	0.27	0.14	HOMO	6.32
B	6.93	0.15	0.27	HOMO-1	6.88
C	7.74	0.43	0.43	HOMO-2	7.40
				HOMO-3	7.57
				HOMO-4	7.85
D	8.40	0.14	0.06	HOMO-5	8.10

[a] Intensities are given relative to the sum of A−D as 1.

[CoCp*(2,5-ᵗBu$_2$PC$_4$H$_2$)] (IE = 8.24, 8.89 eV).[44] This suggests that, in a fashion analogous to that in [NiCp*(2,5-ᵗBu$_2$PC$_4$H$_2$)] and [CoCp*(2,5-ᵗBu$_2$PC$_4$H$_2$)], the P(2) center in **4** is weakly basic.

The relative decrease in intensity of bands A and D relative to that of bands B and C in the He II spectrum indicates that the HOMO and HOMO-5 orbitals that give rise to bands A and D have little metal character. Mulliken population analysis of the ground-state structure of [Ti{N(ᵗBu)PC(ᵗBu)PC(ᵗBu)}(COT)] (**4**) gives the Ti contribution to the HOMO as 3% and to the HOMO-5 as 8%, while the metal contribution to the HOMO-1, HOMO-2, HOMO-3, and HOMO-4 is greater than 15% in all cases. This is consistent with the intensity increase of bands B and C relative to that of bands A and D as the photon energy is increased. Overall, the results of the PES study clearly support the ordering and composition of the MOs that was proposed in the DFT study.

Stability of Products of the Type [Ti{N(R)PC(ᵗBu)PC(ᵗBu)}(COT)]. Results from previous sections indicate that the most stable metal-containing products from the reaction of 2 equiv of ᵗBuC≡P with compounds of the type [Ti(NR)(COT)] have structures similar to those of [Ti{N(ᵗBu)PC(ᵗBu)PC(ᵗBu)}(COT)] (**4**). Although the mechanism for the formation of organic products such as N(Ar)P$_2$C$_2$ᵗBu$_2$ (**6**), which incorporate a 1,2,4-azadiphosphole ring, is unclear, it is possible that compound **6** is formed via a reductive elimination from [Ti{N(Ar)PC(ᵗBu)PC(ᵗBu)}(COT)] (**9**). Reductive elimination of **6** from **9** would also result in the formation of a highly reactive Ti(COT) fragment, which would presumably polymerize or undergo further reaction with solvent. This may explain why no metal-containing products have been isolated from experiments which result in the formation of 1,2,4-azadiphospholes. To investigate the reductive elimination of N(R)P$_2$C$_2$ᵗBu$_2$ and Ti(COT) from compounds of the type [Ti{N(R)PC(ᵗBu)PC(ᵗBu)}(COT)], the structures of [Ti{N(R)PC(ᵗBu)PC(ᵗBu)}(COT)](R = H (**10a**), Me (**10b**), ᵗBu (**4**), Ar (**9**)), N(R)P$_2$C$_2$ᵗBu$_2$ (R = H (**11a**), Me (**11b**), ᵗBu (**11c**), Ar (**6**)), and Ti(COT) were optimized with no symmetry constraints. The optimized structures of **11a**,**c** and **6** are shown in Figure 8, and the relative energies of starting materials and products are compared in Table 7. It should be noted that the same products could be formed as a result of a reductive elimination from compounds such as **4a** and **9a**, but as **4** and **9** are lower in energy than **4a** and **9a**, the energies of reductive elimination from compounds such as **4a** and **9a** have not been studied.

The optimized geometries of compounds **10a**,**b** are comparable to those described earlier for compounds **4** and **9**, with similar bond lengths and angles observed in the TiC$_2$P$_2$N cores of all four molecules (see Figure 5). The structures of the 1,2,4-azadiphosphole rings in compounds **11a**−**c** and **6** are also similar. In compound **6**, the aryl ring on the N atom is oriented perpendicular to the five-membered 1,2,4-azadiphosphole ring. Overall, the calculated bond lengths and angles in the 1,2,4-azadiphosphole rings of compounds **11a**−**c** and **6** are in good agreement with the experimental values observed in the crystallographically characterized compound N(Ph)P$_2$C$_2$ᵗBu$_2$ (see the Supporting Information).[27]

The relative energies in Table 7 indicate that in all cases it is energetically unfavorable to eliminate N(R)P$_2$C$_2$ᵗBu$_2$ from [Ti{N(R)PC(ᵗBu)PC(ᵗBu)}(COT)]. However, given the known instability of the reactive Ti(COT) fragment, this is not surprising (Ti(COT) would almost certainly undergo further reaction immediately in solution). Instead of considering the absolute energies, it is more instructive to examine the trends in the relative energy of the products, as the steric bulk on [Ti{N(R)PC(ᵗBu)PC(ᵗBu)}(COT)] is varied. Clearly, as the steric bulk on [Ti{N(R)PC(ᵗBu)PC(ᵗBu)}(COT)] is increased it becomes more energetically unfavorable to reductively eliminate a 1,2,4-azadiphosphole ring. This is presumably because when the substituents in both the 1- and 2-positions of the 1,2,4-azadiphosphole ring are large, an unfavorable steric clash occurs. This is consistent with a previous study which found that in six-membered rings formed from ᵗBuC≡P fragments, the effect of having two neighboring *tert*-butyl substituents was to destabilize the ring by approximately 90−105 kJ mol^{-1} compared to the parent ring with only H substituents.[39] Importantly, the products from a reductive elimination from **4** lie approximately 55 kJ mol^{-1} higher in energy than the products from a reductive elimination from **9**. This energy difference is large enough to suggest that reductive elimination may occur in one case and not in the other. Thus, it appears that compound **4** is stable toward reductive elimination because it is sterically

(44) Burney, C.; Carmichael, D.; Forissier, K.; Green, J. C.; Mathey, F.; Ricard, L. *Chem. Eur. J.* **2003**, *9*, 2567.

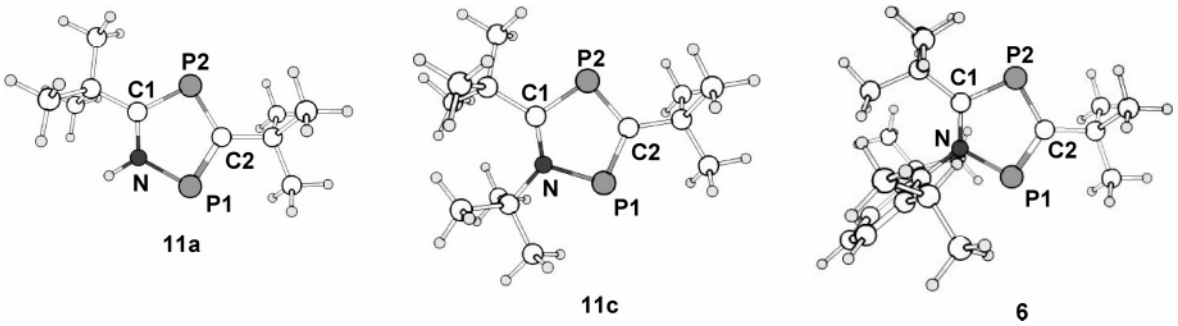

Figure 8. Optimized geometries of $N(R)P_2C_2{}^tBu_2$ (R = H (**11a**), ^{t}Bu (**11c**), Ar (**6**)).

Table 7. Relative SCF Energies[a] of [Ti{N(R)PC(^{t}Bu)PC(^{t}Bu)}(COT)] (R = H (10a), Me (10b), ^{t}Bu (4), Ar (9)), $N(R)P_2C_2{}^tBu_2$ (R = H (11a), Me (11b), ^{t}Bu (11c), Ar (6)), and Ti(COT)

	R	[Ti{N(R)PC(^{t}Bu)PC(^{t}Bu)}(COT)] (kJ mol^{-1})		$N(R)P_2C_2{}^tBu_2$ and Ti(COT) (kJ mol^{-1})
10a	H	0	**11a**	145
10b	Me	0	**11b**	160
4	^{t}Bu	0	**11c**	229
9	Ar	0	**6**	174

[a] In each case the combined SCF energy of [Ti{N(R)PC(^{t}Bu)PC(^{t}Bu)}(COT)] is defined as being 0 kJ mol^{-1}.

unfavorable to form a 1,2,4-azadiphosphole ring with *tert*-butyl substituents in both the 1- and 2-positions.

Conclusions

In this work we have demonstrated the reactivity of the pseudo two-coordinate titanium imido complexes [Ti(N^{t}Bu)(COT)] (**1**), [Ti(N^{t}Bu)(COT″)] (**2**), and [Ti(NAr)(COT)] (**3**) with ^{t}BuC≡P. The imido subsituent is crucial in determining the nature of the products, as the reactions of **1** and **2** with 2 equiv of ^{t}BuC≡P generate the novel complexes [Ti{N(^{t}Bu)PC(^{t}Bu)-PC(^{t}Bu)}(COT)] (**4**) and [Ti{N(^{t}Bu)PC(^{t}Bu)PC(^{t}Bu)}(COT″)] (**5**), respectively, while the reaction of an excess of ^{t}BuC≡P with **3** results in the formation of the organic compound N(Ar)-$P_2C_2{}^tBu_2$ (**6**). Although compound **4** is apparently a 20-electron species, the HOMO is almost entirely ligand-based. Computational studies indicate that the mechanisms for the formation of compounds **4** and **6** probably share several steps. The first step in the reactions of both **1** and **3** with ^{t}BuC≡P is almost certainly a [2 + 2] cycloaddition between the imide and ^{t}BuC≡P to give a four-membered metallacycle with a Ti−C bond. Subsequently, in the reaction between **1** and ^{t}BuC≡P, reaction of another molecule of ^{t}BuC≡P with the four-membered metallacycle yields the product [Ti{N(^{t}Bu)PC(^{t}Bu)PC(^{t}Bu)}-(COT)] (**4**). In the reaction of **3** and ^{t}BuC≡P, it is plausible that a product of the type [Ti{N(Ar)PC(^{t}Bu)PC(^{t}Bu)}(COT)] is formed in a fashion analogous to that for **4**; however, in this case it is energetically favorable for the product to undergo reductive elimination to give **6**. Presumably, compound **4** is stable toward reductive elimination because it is sterically unfavorable to form a 1,2,4-azadiphosphole ring with *tert*-butyl substituents in both the 1- and 2-positions. In the future, we hope to fully explore the range of organic products that can be synthesized through the reactions of titanium imides with phosphaalkynes by further varying both the imido and the phosphaalkyne substituents.

Experimental Section

General Methods and Instrumentation. All manipulations were carried out using standard Schlenk line or drybox techniques under an atmosphere of argon or dinitrogen. Solvents were predried over activated 4 Å molecular sieves, refluxed over appropriate drying agents under a dinitrogen atmosphere, and collected by distillation. Deuterated solvents were dried over appropriate drying agents, distilled under reduced pressure, and stored under dinitrogen in Teflon valve ampules. NMR samples were prepared under dinitrogen in 5 mm Wilmad 507 NMR tubes fitted with J. Young Teflon valves. ^{1}H, ^{13}C, and ^{31}P spectra were recorded on Varian Unity Plus 300, Bruker DPX 300, or Bruker AMX 500 spectrometers. ^{1}H and ^{13}C assignments were confirmed when necessary with the use of NOE and two-dimensional ^{1}H−^{1}H and ^{13}C−^{1}H NMR experiments. ^{1}H and ^{13}C NMR spectra were referenced internally to residual solvent resonances and are reported relative to tetramethylsilane (δ 0 ppm), while ^{31}P NMR spectra were referenced to external neat H_3PO_4 at δ 0 ppm. Chemical shifts are quoted in δ (ppm) and coupling constants in hertz. Infrared spectra were prepared as Nujol mulls between NaCl plates and were recorded on Perkin-Elmer 1600 and 1700 series spectrometers. Infrared data are quoted in wavenumbers (cm^{-1}). Mass spectra were recorded by either the mass spectrometry service of the University of Oxford's Inorganic Chemistry Laboratory or at the University of Sussex. Combustion analyses were recorded by the analytical services at the London Metropolitan University.

PE spectra were measured using a Helectros 0078 spectrometer with a He discharge lamp capable of producing both He I and He II spectra. The spectrometer was interfaced with an Atari processor, which enabled spectral acquisition by repeated scans. The samples were calibrated using He, Xe, and N_2, and band intensities were estimated using the Gaussian fitting program available in the IGOR program suite. Band positions and widths were obtained by a free fit to the He I spectra and were maintained at the same IE for the lower resolution He II spectra.

Density functional calculations were performed using either Gaussian 03[45] or ADF version 2004.01[46−48] to take advantage of

(45) Frisch, M. J.; Trucks, G. W.; Schlegel, H. B.; Scuseria, G. E.; Robb, M. A.; Cheeseman, J. R.; Montgomery, J. A., Jr.; Vreven, T.; Kudin, K. N.; Burant, J. C.; Millam, J. M.; Iyengar, S. S.; Tomasi, J.; Barone, V.; Mennucci, B.; Cossi, M.; Scalmani, G.; Rega, N.; Petersson, G. A.; Nakatsuji, H.; Hada, M.; Ehara, M.; Toyota, K.; Fukuda, R.; Hasegawa, J.; Ishida, M.; Nakajima, T.; Honda, Y.; Kitao, O.; Nakai, H.; Klene, M.; Li, X.; Knox, J. E.; Hratchian, H. P.; Cross, J. B.; Bakken, V.; Adamo, C.; Jaramillo, J.; Gomperts, R.; Stratmann, R. E.; Yazyev, O.; Austin, A. J.; Cammi, R.; Pomelli, C.; Ochterski, J. W.; Ayala, P. Y.; Morokuma, K.; Voth, G. A.; Salvador, P.; Dannenberg, J. J.; Zakrzewski, V. G.; Dapprich, S.; Daniels, A. D.; Strain, M. C.; Farkas, O.; Malick, D. K.; Rabuck, A. D.; Raghavachari, K.; Foresman, J. B.; Ortiz, J. V.; Cui, Q.; Baboul, A. G.; Clifford, S.; Cioslowski, J.; Stefanov, B. B.; Liu, G.; Liashenko, A.; Piskorz, P.; Komaromi, I.; Martin, R. L.; Fox, D. J.; Keith, T.; Al-Laham, M. A.; Peng, C. Y.; Nanayakkara, A.; Challacombe, M.; Gill, P. M. W.; Johnson, B.; Chen, W.; Wong, M. W.; Gonzalez, C.; Pople, J. A. *Gaussian 03*, revision C.02; Gaussian, Inc.: Wallingford, CT, 2004.

(46) te Velde, G.; Bickelhaupt, F. M.; Baerends, E. J.; Fonseca Guerra, C.; Van Gisbergen, S. J. A.; Snijders, J. G.; Ziegler, T. *J. Comput. Chem.* **2001**, *22*, 931.

(47) Fonseca Guerra, C.; Snijder, J. G.; Te Velde, G.; Baerends, E. J. *Theor. Chem. Acc.* **1998**, *99*, 391.

(48) ADF2004.01; SCM, Theoretical Chemistry, Vrije Universiteit, Amsterdam, The Netherlands; http://www.scm.com.

the technical differences in these software packages. Gaussian was used to optimize geometries, perform frequency calculations, and search for transition states. ADF was employed for fragment calculations in order to determine the bonding in the stationary points found and also to calculate NMR chemical shifts and ionization energies. All energies quoted are SCF energies and do not take into account solvent or entropy effects.

Gaussian 03 calculations were performed using the density functional/Hartree−Fock hybrid B3LYP.[49−52] Optimizations and frequency calculations were performed using the Stuttgart−Dresden[53,54] basis set for Ti and P atoms and the 6-31G** basis set for all other atoms. Transition states were found using the QST2/QST3 method, and all stationary points were verified using frequency calculations. IRC calculations were carried out to verify that the transition states found were correct saddle points connecting the proposed minima. Distances and angles from the optimized structures in IRC calculations were within 0.02 Å and 2.5° of the proposed minima.

In all ADF calculations the generalized gradient approximation was employed, using the local density approximation of Vosko, Wilk, and Nusair[49] together with the nonlocal exchange correction by Becke[52,55] and nonlocal correlation corrections by Perdew.[56] In single-point calculations TZP basis sets were used with triple-ζ accuracy sets of Slater type orbitals and a single polarization function added to the main-group atoms. The cores of the atoms were frozen up to 1s for C and N and 2p for Ti and P. Fragment analyses used the MOs of the chosen fragments as the basis set for the molecular calculation. Initial spin-restricted calculations were carried out on the fragments with the geometry that they had in the molecule; thus, the fragments were in a prepared singlet state. In NMR calculations all-electron TZ2P basis sets were used with triple-ζ accuracy sets of Slater type orbitals and two polarization functions added to all atoms. The ^{13}C and ^{31}P NMR shielding tensors were computed using the NMR program[57−61] incorporated in ADF version 2004.01. The magnetic shielding tensors of the C atom in optimized $SiMe_4$ and the P atom in optimized PH_3 were evaluated using the same procedure to serve as a reference for the calculation of ^{13}C and ^{31}P NMR chemical shifts. Chemical shifts were calculated using the formula

$$\delta(\text{calcd}) = \sigma_{\text{ref}}(\text{calcd}) + \delta_{\text{ref}}(\text{calcd}) - \sigma_{\text{unknown}}(\text{calcd})$$

where δ_{ref}(calcd) was 0 ppm for the C atom in $SiMe_4$ and −266.1 ppm for the P atom in PH_3.

Literature Preparations. [Ti(N^{t}Bu)(COT)] (**1**),[28] [Ti(N^{t}Bu)(COT″)] (**2**),[28] [Ti(NAr)(COT)] (**3**),[28] and ^{t}BuC≡P[62] were prepared using literature methods.

Synthesis of [Ti{N(^{t}Bu)PC(^{t}Bu)PC(^{t}Bu)}(COT)] (4). To a stirred and cooled solution of [Ti(N^{t}Bu)(COT)] (**1**; 0.51 g, 2.3 mmol) in toluene (20 mL, −50 °C) was added dropwise ^{t}BuC≡P (0.46 g, 4.6 mmol). Upon addition of ^{t}BuC≡P the orange solution turned dark brown. The reaction mixture was warmed to room temperature and stirred for 24 h. Removal of the solvent in vacuo and recrystallization from pentane yielded **4** as dark brown crystals. Yield: 0.70 g (71%). Crystals suitable for X-ray analysis were grown by slowly cooling (−18 °C) a concentrated pentane solution.

^{1}H NMR (C_6D_6, 300.0 MHz, 295 K): δ 6.10 (8H, s, C_8H_8), 1.26 (9H, s, NC(CH_3)$_3$), 1.10 (18H, s, PCC(CH_3)$_3$). ^{13}C{^{1}H} NMR (C_6D_6, 75.5 MHz): δ 185.3 (m, P*C*CCH$_3$), 96.3 (C_8H_8), 61.2 (d, N*C*(CH$_3$)$_3$, $^2J_{C-P}$ 12.5 Hz), 39.3 (pseudo-t, PC*C*(CH$_3$)$_3$, $^3J_{C-P}$ = 8.2 Hz), 34.7 (pseudo-t, PCC(*C*H$_3$)$_3$, $^3J_{C-P}$ = 5.6 Hz), 34.3 (d, NC(*C*H$_3$)$_3$, $^3J_{C-P}$ = 11.7 Hz). ^{31}P{^{1}H} NMR (C_6D_6, 121.5 MHz, 295 K): δ 215.4 (d, ^{t}BuNPC(^{t}Bu)*P*C(^{t}Bu), $^2J_{P-P}$ = 38.7 Hz), −190.8 (d, ^{t}BuN*P*C(^{t}Bu)PC(^{t}Bu)). IR (NaCl plates, Nujol mull, cm^{-1}): 1260 (sh, m), 1193 (br, m), 1091 (br, m), 1055 (br, s), 1022 (br, s), 802 (m), 726 (s). EI-MS: *m*/*z* 423 (M)$^+$, 408 (M − Me)$^+$. Anal. Found (calcd for $C_{22}H_{35}NP_2Ti$): C, 62.3 (62.4); H, 8.4 (8.3).

Synthesis of [Ti{N(^{t}Bu)PC(^{t}Bu)PC(^{t}Bu)}(COT″)] (5). To a stirred solution of [Ti(N^{t}Bu)(COT″)] (**2**; 0.25 g, 0.68 mmol) in toluene (10 mL) was added ^{t}BuC≡P (0.14 g, 1.3 mmol). Upon addition of ^{t}BuC≡P the yellow solution turned dark brown. The reaction mixture was stirred for 24 h, and the volatiles were removed under reduced pressure to give a black residue. The black residue was recrystallized from pentane to give **5** as a dark brown powder. Yield: 0.29 g (75%).

^{1}H NMR (C_6D_6, 300.0 MHz, 298 K): δ 6.30 (2H, s, 2- and 3-$C_8H_6(SiMe_3)_2$), 6.29 (2H, m, 5- and 8-$C_8H_6(SiMe_3)_2$), 6.21 (2H, m, 6- and 7-$C_8H_6(SiMe_3)_2$), 1.34 (9H, d, NC(CH_3)$_3$, $^4J_{H-P}$ = 3.8 Hz), 1.43 (18H, s, PCC(CH_3)$_3$), 0.43 (18H, s, $SiMe_3$). ^{13}C{^{1}H} NMR (C_6D_6, 75.5 MHz, 298 K): δ 183.3 (dd, P*C*^{t}Bu, $^1J_{C-P}$ = 24.5 Hz, $^1J_{C-P}$ = 62.2 Hz), 107.8 (1- and 4-*C*$_8$H$_6$(SiMe$_3$)$_2$), 105.6 (5- and 8-*C*$_8$H$_6$(SiMe$_3$)$_2$), 98.4 (2- and 3-*C*$_8$H$_6$(SiMe$_3$)$_2$), 94.6 (6- and 7-*C*$_8$H$_6$(SiMe$_3$)$_2$), 61.7 (d, N*C*Me$_3$, $^2J_{C-P}$ = 13.0 Hz), 39.5 (pseudo-t, PC*C*Me$_3$, $^2J_{C-P}$ = 8.4 Hz), 34.9 (pseudo-t, PC*C**Me*$_3$, $^2J_{C-P}$ = 5.3 Hz), 34.5 (d, NC*Me*$_3$, $^3J_{C-P}$ = 6.1 Hz), 0.5 (Si*Me*$_3$). ^{31}P{^{1}H} NMR (C_6D_6, 121.5 MHz, 298 K): δ 216.9 (d, ^{t}BuNPC(^{t}Bu)*P*C(^{t}Bu), $^2J_{P-P}$ = 39.6 Hz), −192.9 (d, ^{t}BuN*P*C(^{t}Bu)PC(^{t}Bu), $^2J_{P-P}$ = 39.6 Hz). IR (NaCl plates, Nujol mull, cm^{-1}): 2375 (w), 2345 (w), 1618 (br, m), 1193 (br, s), 1091 (br, s), 1055 (br, s), 1019 (br, s), 836 (m), 799 (s). EI-MS: *m*/*z* 600 (M)$^+$, 510 (M − 6Me)$^+$, 454 (M − 2SiMe$_3$)$^+$, 398 (M − 2SiMe$_3$ and ^{t}Bu)$^+$, 296 (Ti(COT″))$^+$, 73 (SiMe$_3$)$^+$. Anal. Found (calcd for $C_{26}H_{51}NP_2Si_2Ti$): C, 57.5 (57.4); H, 9.4 (9.5); N, 2.6 (2.6).

Synthesis of N(Ar)P$_2$C$_2$^{t}Bu$_2$ (6). To a stirred solution of [Ti(NAr)(COT)] (**3**; 0.25 g, 0.76 mmol) in toluene (10 mL) was added ^{t}BuC≡P (0.31 g, 3.0 mmol). Upon addition of ^{t}BuC≡P the yellow solution turned dark brown. The reaction mixture was heated with stirring for 3 days at 60 °C. The volatiles were removed under reduced pressure to give a dark brown residue. The residue was extracted with ether (15 mL) and the solution filtered. The solvent was again removed under reduced pressure to give a brown solid. The solid was sublimed (80 °C, 1 × 10^{-4} mbar) to afford **6** as an off-white powder. Yield: 0.086 g (30%).

^{1}H NMR (C_6D_6, 300.0 MHz, 298 K): δ 7.14 (1H, partially obscured d, para NAr), 6.99 (2H, d, meta NAr, $^3J_{H-H}$ = 7.9), 2.54 (2H, sept, C*H*Me$_2$, $^3J_{H-H}$ = 6.7 Hz), 1.65 (9H, d, PC^t*Bu*P, $^4J_{H-P}$ = 1.2 Hz), 1.33 (9H, d, PC^t*Bu*N, $^4J_{H-P}$ = 1.9 Hz), 1.20 (6H, d, CH*Me*$_2$, $^3J_{H-H}$ = 6.7 Hz, 6H), 1.19 (6H, d, $^3J_{H-H}$ = 6.7 Hz, CH*Me*$_2$). ^{13}C{^{1}H} NMR (C_6D_6, 75.5 MHz, 298 K): δ 203.6 (dd, P*C*P, $^1J_{C-P}$ = 58.0 Hz, $^1J_{C-P}$ = 62.4 Hz), 196.0 (d, br, N*C*P, $^1J_{C-P}$ = 57.1 Hz), 139.2 (d, *ipso*-NAr, $^2J_{C-P}$ = 15.1 Hz), 129.6 (d, ortho NAr, $^3J_{C-P}$ = 3.0 Hz), 127.9 (para NAr), 123.8 (meta NAr), 40.1 (dd, NC(*C*Me$_3$)P, $^2J_{C-P}$ = 18.9 Hz, $^4J_{C-P}$ = 3.8 Hz), 37.4 (pseudo-t, PC(*C*Me$_3$)P, $^2J_{C-P}$ = 21.3 Hz), 35.5 (dd, PC(C*Me*$_3$)P, $^3J_{C-P}$ = 13.0 Hz, $^3J_{C-P}$ = 18.0 Hz), 33.3 (d, NC(C*Me*$_3$)P, $^3J_{C-P}$ = 21.9 Hz), 29.0 (CH*Me*$_2$), 22.5 (*C*HMe$_2$), 22.1 (CH*Me*$_2$). ^{31}P{^{1}H} NMR (C_6D_6,

(49) Vosko, S. H.; Wilk, L.; Nusair, M. *Can. J. Phys.* **1980**, *58*, 1200.
(50) Stephens, P. J.; Devlin, F. J.; Chabalowski, C. F.; Frisch, M. J. *J. Phys. Chem.* **1994**, *98*, 11623.
(51) Lee, C.; Yang, W.; Parr, R. G. *Phys. Rev. B: Condens. Matter Mater. Phys.* **1988**, *37*, 785.
(52) Becke, A. D. *J. Chem. Phys.* **1988**, *88*, 1053.
(53) Andrae, D.; Häussermann, U.; Dolg, M.; Stoll, H.; Preuss, H. *Theor. Chim. Acta* **1990**, *77*, 123.
(54) Bergner, A.; Dolg, M.; Küchle, W.; Stoll, H.; Preuss, H. *Mol. Phys.* **1993**, *80*, 1431.
(55) Becke, A. D. *Phys. Rev. A: At., Mol., Opt. Phys.* **1988**, *38*, 3098.
(56) Perdew, J. P. *Phys. Rev. B* **1986**, *33*, 8800.
(57) Schreckenbach, G.; Ziegler, T. *J. Phys. Chem.* **1995**, *99*, 606.
(58) Schreckenbach, G.; Ziegler, T. *Int. J. Quantum Chem.* **1996**, *60*, 753.
(59) Schreckenbach, G.; Ziegler, T. *Int. J. Quantum Chem.* **1997**, *61*, 899.
(60) Wolff, S. K.; Ziegler, T. *J. Chem. Phys.* **1998**, *109*, 895.
(61) Wolff, S. K.; Ziegler, T.; van Lenthe, E.; Baerends, E. J. *J. Chem. Phys.* **1999**, *110*, 7689.
(62) Becker, G.; Schmidt, H.; Uhl, G.; Uhl, W. *Inorg. Synth.* **1990**, *27*, 249.

Table 8. Crystal Data Collection and Processing Parameters for [Ti{N(ᵗBu)PC(ᵗBu)PC(ᵗBu)}(COT)] (4)

empirical formula	$C_{22}H_{35}NP_2Ti$
fw	423.35
temp/K	175(2)
wavelength/Å	0.710 73
space group	$P2_1/c$
a (Å)	14.054(6)
b (Å)	10.190(4)
c (Å)	15.592(2)
α (deg)	90
β (deg)	93.90(3)
γ (deg)	90
V (Å^3)	2228(1)
Z	4
D(calcd) (Mg m^{-3})	1.26
abs coeff (mm^{-1})	0.53
R indices ($I > 2\sigma(I)$)	R1 = 0.040 wR2 = 0.089

121.5 MHz, 298 K): *δ* 260.0 (d, NPC(ᵗBu)*P*C(ᵗBu), $^2J_{P-P}$ = 29.2 Hz), 154.6 (d, N*P*C(ᵗBu)PC(ᵗBu)). IR (NaCl plates, Nujol mull, cm^{-1}): 1260 (s), 1090 (br, s), 1020 (s), 807 (s), 831 (m), 722 (m). EI-MS: *m*/*z* 375 (M)$^+$, 360 (M − Me)$^+$, 318 (M − ᵗBu)$^+$, 261 (M − 2ᵗBu)$^+$, 57 (ᵗBu)$^+$. HR EI-MS for N(Ar)P_2C_2ᵗBu_2: found (calcd for $C_{22}H_{35}NP_2$) *m*/*z* 375.2239 (375.2245). Anal. Found (calcd for $C_{22}H_{35}NP_2$): C, 70.3 (70.4); H, 9.4 (9.4); N, 3.7 (3.7).

Crystal Structure Determination of [Ti{N(ᵗBu)PC(ᵗBu)PC(ᵗBu)}(COT)] (4). Crystal data collection and processing parameters are given in Table 8. Crystals were mounted on a glass fiber using perfluoropolyether oil and cooled rapidly to 175 K under a stream of cold N_2 using an Oxford Cryosystems CRYOSTREAM unit. Diffraction data were measured using an Enraf-Nonius CAD-4 diffractometer, and intensity data were processed using the Enraf-Nonius CAD4 software.[63] The structures were solved using SHELXS-86,[64] which located all non-hydrogen atoms. Subsequent full-matrix least-squares refinement was carried out using the SHELXL-93 program suite.[65] Coordinates and anisotropic thermal parameters of all non-hydrogen atoms were refined. Hydrogen atoms were positioned geometrically, and weighting schemes were applied as appropriate. Full listings of atomic coordinates, bond lengths and angles, and displacement parameters are provided in the Supporting Information.

Acknowledgment. This work was supported by funding from the EPSRC and Rhodes Trust. We thank Professors E. Clot and J. D. Protasiewicz for valuable advice and discussions. Calculations were carried out using the facilities of the Oxford Supercomputing Centre or the EPSRC National Service for Computational Chemistry Software. URL: http://www.nsccs.ac.uk.

Supporting Information Available: X-ray crystallographic data as a CIF file for the structure determination of **4** and tables and figures giving further details of the DFT calculations. This material is available free of charge via the Internet at http://pubs.acs.org.

OM060273O

(63) Enraf-Nonius CAD4 Software, Version 5.0; Enraf-Nonius, 1989.
(64) Sheldrick, G. M. *Acta Cyrstallogr., Sect. A* **1990**, *46*, 467.
(65) Sheldrick, G. M. SHELXL 96; Institut für Anorganische Chemie der Universität Göttingen, Göttingen, Germany, 1996.